Electronic Supplementary Material (ESI) for ChemComm.

A Radically Coupled Pathway to a Stable and Terminally Bound Titanium Methylidene.

Takashi Kurogi,[‡] Patrick J. Carroll,[‡] and Daniel J. Mindiola*[‡]

[‡]*Department of Chemistry, University of Pennsylvania, 231 South 34th Street, Philadelphia, Pennsylvania 19104*

Table of contents

General Procedure

All operations were performed in a M. Braun glove box or using standard Schlenk techniques under a nitrogen atmosphere unless otherwise stated. Anhydrous solvents were purchased from Fisher Scientific or Aldrich. All anhydrous solvents (pentane, hexane, toluene and benzene) were purified and dried by passage through two columns of activated alumina and Q-5 drying agent in a Grubbs-type solvent system. Stabilizer-free ethereal solvents (Et_2O and THF) and pyridine were purchased from Fisher Scientific and dried by passage through two columns of activated alumina. All bulk solvents were kept over sodium and 4 Å molecular sieves. Benzene-d_6 (Cambridge Isotope Laboratories) was dried and degassed over a potassium mirror prior to use. Celite and 4 Å molecular sieves were activated under vacuum overnight at 200 °C. Li(PNP),[1] $TiCl_3(THF)_3$,[2] phenoxyl radical (•OMes*, Mes* = 2,4,6-^{t}Bu$_3$C$_6$H$_2$),[3] and $[FeCp_2][OTf]$[4] were prepared according to the reported procedures. TEMPO was purchased from Aldrich and purified by sublimation under vacuum at 50 °C. $^{13}CH_3I$ (99 atom % ^{13}C) was purchased from Aldrich. All other chemicals were purchased from commercial sources and degassed before being used. ^1H, ^{13}C, ^{19}F, ^{31}P, HMQC, HMBC and EXSY NMR spectra were recorded on a Bruker AV-II 500 MHz, AV-III 400 MHz or DMX 300 MHz spectrometers. ^1H and ^{13}C NMR chemical shifts are reported referenced to the internal residual proton or carbon resonances of C_6D_6 (δ = 7.16 ppm or 128.06 ppm). ^{19}F and ^{31}P NMR chemical shifts are reported with respect to external CF_3CO_2H (δ –78.5 ppm) and H_3PO_4 (δ 0.0 ppm), respectively. Solution state magnetic susceptibility was measured by Evans' method[5] in benzene-d_6/pyridine/tetramethylsilane. Corrections were applied for diamagnetism calculated for Pascal constants.[6] Elemental analyses were performed at a FLASH EA 1112 Series CHN analyzer (Thermo Finnigan). Photolysis experiments were performed by a MAX-303 Xe-lamp photoreactor (Asahi Spectra Company) equipped with a UV mirror module (250-385 nm).

Synthesis of [(PNP)Ti(CH_3)$_2$] (1)

To a blue suspension of $TiCl_3(THF)_3$ (425 mg, 1.15 mmol) in toluene (10 mL) was added Li(PNP) (500 mg, 1.15 mmol) as solid at room temperature and additional toluene (10 mL) was used to add the remainder of Li(PNP). After stirring for 5 h, the reaction mixture changed color to a dark brown suspension/solution containing (PNP)$TiCl_2$.[7] To the dark brown mixture of (PNP)$TiCl_2$ and LiCl was added H_3CMgCl in THF (3.0 M, 0.76 mL, 2.28 mmol) and 1,4-dioxane (0.70 mL) via a syringe at −35 °C, resulting in a color change to greenish. After stirring for 2 h, the reaction mixture was evaporated to dryness. The gray residue was extracted into toluene (50 mL) and the greenish suspension was filtered through a medium porosity glass frit containing Celite. The Celite was washed twice with toluene (2 × 20 mL). The green filtrate was evaporated to dryness and the residue was washed twice with pentane (2 × 3 mL) to yield **1** as green solid (308 mg, 608 μmol, 53% yield).

^{1}H NMR (400 MHz, benzene-d_6, 300 K): δ 9.63 (br, 6H, $\Delta\nu_{1/2}$ = 48 Hz), 7.04 (br, 2H, overlapped with C_6D_5H), 6.55 (br, 2H, $\Delta\nu_{1/2}$ = 43 Hz), 5.12 (br, 2H, $\Delta\nu_{1/2}$ = 25 Hz), 3.97 (br, 6H, $\Delta\nu_{1/2}$ = 59 Hz), 2.54 (br, 6H, $\Delta\nu_{1/2}$ = 16 Hz), 2.28 (br, 2H, $\Delta\nu_{1/2}$ = 9 Hz), 2.11 (br, 2H), 1.26, 0.99, 0.89 (overlapped br, 18H). μ_{eff} (Evans' Method, benzene-d_6/pyridine, 300 K): 1.82 μ_B. Anal. Calcd. for $C_{28}H_{46}NP_2Ti$: C, 66.40; H, 9.15; N, 2.77. Found: C, 66.52; H, 8.71; N, 2.41.

Synthesis of [(PNP)Ti(CH_3)$_2$(TEMPO)] (2)

To a green suspension of **1** (200 mg, 395 μmol) in toluene (10 mL) was added TEMPO (63.1 mg, 420 μmol) in toluene (5 mL) at −35 °C, resulting in a color change to orange. After stirring for 30 min at room temperature, the reaction mixture was filtered through glass wool in a pipette. The orange filtrate was evaporated to dryness under reduced pressure. The residue was triturated with pentane (3 mL) to yield **2** as yellowish orange powder (197 mg, 297 μmol, 75% yield). Orange crystals suitable for X-ray analysis were

grown from concentrated pentane solution at −35 °C.

^{1}H NMR (400 MHz, benzene-d_6, 300 K): δ 7.18 (br, 2H, Ar-C*H*), 7.01 (d, 2H, *J* = 10Hz, Ar-C*H*), 6.74 (br, 2H, Ar-C*H*), 2.53 (br, 4H, PC*H*$(CH_3)_2$), 2.18 (s, 6H, ArCH_3), 1.48 (br d, 3H, PCH(CH_3)$_2$) 1.39 (s, 12H, TEMPO-CH_3), 1.30 (s, 12H, TEMPO-CH_2), 1.4-1.1 (overlapped br, 21H, PCH(CH_3)$_2$). Ti-CH_3 was assigned at δ 2.07 by HMQC and HMBC experiments of **2-^{13}C**. ^{13}C{^{1}H} NMR (126 MHz, benzene-d_6, 300 K) δ. 133.47 (PNP-Ar), 131.78 (PNP-Ar), 129.34 (PNP-Ar), 62.30 (TEMPO-CH_2), 60.20 (br, TEMPO-N*C*$(CH_3)_2$), 40.10 (TEMPO), 27.32 (br, TEMPO-CH_3), 24.09 (br, P*C*H$(CH_3)_2$), 20.83 (br, PCH(*C*H_3)$_2$), 19.28 (Ar*C*H_3), 17.31 (TEMPO-CH_2). Fluxional behavior in solution prevented up from measuring ^{13}C signals in the PNP ligand's aromatic rings. Ti-CH_3 was assigned at δ 60.4 by ^{13}C NMR of **2-^{13}C**. ^{31}P{^{1}H} NMR (162 MHz, benzene-d_6, 300 K) δ 11.48 (br, PNP), –2.33 (br, PNP). Anal. Calcd. for $C_{34}H_{64}N_2OP_2Ti$: C, 67.06; H, 9.73; N, 4.23. Found: C, 67.26; H, 10.01; N, 4.10.

Synthesis of [(PNP)Ti$(CH_3)_2$(OMes*)] (3)

To a green suspension of **1** (200 mg, 395 μmol) in toluene (10 mL) was added •OMes* (111 mg, 425 μmol) dissolved in toluene (5 mL) at –35 °C with vigorous stirring. The color of the reaction mixture gradually changed from the unreacted blue-green to dark brown. After stirring for 3 h at room temperature, the reaction mixture was filtered through glass wool in a pipette. The brown filtrate was evaporated to dryness under reduced pressure. The residue was triturated with pentane (3 mL) to yield **3** as yellowish brown powder (231 mg, 301 μmol, 76% yield).

^{1}H NMR (400 MHz, benzene-d_6, 300 K): δ 7.53 (br, 1H, Ar-C*H*), 7.47 (br, 1H, Ar-C*H*), 7.27 (br, 1H, Ar-C*H*), 7.03 (br, 1H, Ar-C*H*), 6.98 (br, 1H, Ar-C*H*), 6.70 (br, 1H, Ar-C*H*), 6.67 (br, 1H, Ar-C*H*), 5.75 (br, 1H, Ar-C*H*), 4.05 (br, 1H, PC*H*$(CH_3)_2$), 2.71 (br, 1H, PC*H*$(CH_3)_2$), 2.14 (br s, 3H, ArCH_3), 2.12 (br s, 3H, ArCH_3), 2.05 (br d, $^{3}J_{HP}$ = 10 Hz, 3H, Ti-CH_3), 1.70 (br, 3H, Ti-CH_3), 1.69 (br, 3H, PCH(CH_3)$_2$), 1.62 (overlapped br, 4H,

PC*H*(CH_3)$_2$ and PCH(C*H*$_3$)$_2$), 1.45 (br s, 18H, ^{t}Bu), 1.40 (br, PCH(C*H*$_3$)$_2$, 3H), 1.23 (overlapped br, 12H, ^{t}Bu and PCH(C*H*$_3$)$_2$), 1.09 (br, 3H, PCH(C*H*$_3$)$_2$), 0.93 (br, 3H, PCH(C*H*$_3$)$_2$). ^{13}C{^{1}H} NMR (126 MHz, benzene-d_6, 300 K) δ. 164.4 (Ar), 152.0 (Ar), 141.4 (Ar), 135.5 (Ar), 134.6 (Ar), 134.3 (Ar), 133.4 (Ar), 132.8 (Ar), 132.7 (Ar), 132.5 (Ar), 131.3 (Ar), 131.1 (Ar), 128.6 (Ar), 122.3 (Ar), 122.0 (Ar), 82.9 (d, $^2J_{CP}$ = 12 Hz, Ti-*C*H$_3$), 56.4 (d, $^2J_{CP}$ = 10 Hz, Ti-*C*H$_3$), 36.1 (*C*(CH$_3$)$_3$), 34.9 (P*C*H(CH$_3$)$_2$), 34.7 (P*C*H(CH$_3$)$_2$), 33.1 (*C*(CH$_3$)$_3$), 32.7 (P*C*H(CH$_3$)$_2$), 32.4 (P*C*H(CH$_3$)$_2$), 32.1 (C(*C*H$_3$)$_3$), 32.0 (C(*C*H$_3$)$_3$), 31.2 (*C*(CH$_3$)$_3$), 30.6 (C(*C*H$_3$)$_3$), 22.0 – 16.0 (overlapped, Ar-*C*H$_3$, PCH(*C*H$_3$)$_2$). Broadening and overlapping of the ^{13}C{^{1}H} NMR spectrum prevent us from measuring some ^{13}C signals of apical positions on the PNP ligands. ^{31}P{^{1}H} NMR (162 MHz, benzene-d_6, 300 K) δ 26.79 (PNP), -8.21 (PNP). Anal. Calcd. for $C_{46}H_{75}NOP_2Ti$: C, 71.95; H, 9.84; N, 1.82. Found: C, 71.05; H, 8.94; N, 1.60. Multiple attempts to obtain satisfactory elemental analysis data failed.

Synthesis of [(PNP)Ti(CH$_3$){ONC$_5$H$_6$(CH$_3$)$_3$(CH$_2$)}] (4)

A reddish orange solution of **2** (170 mg, 257 μmol) in toluene (15 mL) was placed in a 100 mL J-Young tube. The solution was stirred at 60 °C in the absence of light and the reaction mixture changed in color to yellowish orange. After stirring for 6 h, all volatile materials were removed in vacuo. The residue was triturated twice with cold pentane (−35 °C, 2 × 2 mL) to give **4** as yellow powder (122 mg, 189 μmol, 74% yield).

^{1}H NMR (400 MHz, benzene-d_6, 300 K): δ 7.34 – 7.20 (m, 3H, Ar-C*H*), 7.01 (br d, *J* = 7 Hz, 1H, Ar-C*H*), 6.97 (br d, *J* = 6 Hz, 1H, Ar-C*H*), 6.32 (br d, *J* = 8 Hz, 1H, Ar-C*H*), 6.87-6.84 (overlapped d and br, 3H, Ar-C*H*), 4.86 (d, $^3J_{CP}$ = 11 Hz, Ti-C*H*$_2$), 2.61 (s, 3H, Ti-C*H*$_3$), 2.34-2.17 (m, 2H, PC*H*(CH$_3$)$_2$), 2.19 (s, 3H, ArC*H*$_3$), 2.17 (s, 3H, ArC*H*$_3$), 1.90 (m, 1H, PC*H*(CH$_3$)$_2$), 1.73 (s, 3H, TEMPO-C*H*$_3$), 1.50 (s, 3H, TEMPO-C*H*$_3$), 1.54 (s, 3H, TEMPO-C*H*$_3$), 1.57 – 0.86 (m, 25H, PC*H*(CH$_3$)$_2$ and PCH(C*H*$_3$)$_2$). ^{13}C{^{1}H} NMR (126 MHz, benzene-d_6, 300 K) δ.146.2 (PNP-Ar), 132.8 (PNP-Ar), 132.7 (PNP-Ar), 132.2

(PNP-Ar), 128.3 (PNP-Ar), 127.0 (PNP-Ar), 125.9 (PNP-Ar), 120.0 (d, $^2J_{CP}$ = 7 Hz, PNP-Ar), 117.6 (d, $^2J_{CP}$ = 7 Hz, PNP-Ar), 110.4 (Ti-*C*H_2), 59.6 (N-*C*(CH_3)), 43.4 (CH_2), 39.1 (CH_2), 30.0 (Ti-*C*H_3), 28.8 (N-C(*C*H_3), 28.5 (N-C(*C*H_3), 25.3 (P*C*H(CH_3)$_2$), 24.3 (P*C*H(CH_3)$_2$), 24.0 (P*C*H(CH_3)$_2$), 22.6, 20.9 (Ar*C*H_3), 20.8 (Ar*C*H_3), 20.1 (PCH(*C*H_3)$_2$), 19.7 (PCH(*C*H_3)$_2$), 19.3 (PCH(*C*H_3)$_2$), 18.9 (PCH(*C*H_3)$_2$), 17.2 (CH_2), 16.4 (CH_2). Broadening and overlapping of the $^{13}C\{^1H\}$ NMR spectrum prevent us from measuring some ^{13}C signals of apical positions on the PNP ligand. $^{31}P\{^1H\}$ NMR (162 MHz, benzene-d_6, 300 K) δ 20.48 (d, $^2J_{PP}$ = 57 Hz, PNP), 15.68 (d, $^2J_{PP}$ = 57 Hz, PNP). Anal. Calcd. for $C_{36}H_{60}N_2OP_2Ti$: C, 66.86; H, 9.35; N, 4.33. Found: C, 67.02; H, 9.54; N, 4.10.

Synthesis of [(PNP)Ti(=CH_2)(OMes*)] (5)

A dark reddish brown solution of **3** (260 mg, 342 μmol) in toluene (15 mL) was placed in a 100 mL J-Young tube. The solution was stirred at 70 °C in the absence of light and the reaction mixture changed in color to yellowish brown. After stirring for 6 h, all volatile materials were removed in vacuo. The residue was triturated twice with cold pentane (−35 °C, 2 × 2 mL) to give **5** as yellowish brown powder (218 mg, 290 μmol, 86% yield). ^1H NMR (400 MHz, benzene-d_6, 300 K): δ 14.20 (s, 2H, Ti=C*H*$_2$), 7.57 (overlapped d, 1H, Ar-C*H*), 7.56 (s, 1H, Ar-C*H*), 7.38 (d, $^4J_{HH}$ = 2 Hz, 1H, Ar-C*H*), 7.39 (dd, $^3J_{HH}$ = 8 Hz, $^4J_{HH}$ = 2 Hz, 1H, Ar-C*H*), 7.12 (overlapped dd with C_6D_5H, 1H, Ar-C*H*), 6.97 (br d, 1H, Ar-C*H*), 6.95 – 6.82 (m, 2H, Ar-C*H*), 2.30 (m, 1H, PC*H*(CH_3)$_2$), 2.18 (s, 3H, Ar-C*H*$_3$), 2.13 (s, 3H, Ar-C*H*$_3$), 2.20 – 2.10 (m, 2H, PC*H*(CH_3)$_2$), 1.99 (m, 1H, PC*H*(CH_3)$_2$), 1.75 (br s, 9H, ^{t}Bu), 1.45 (br s, 18H, ^{t}Bu), 1.60 – 1.35, 1.30 – 0.80 (m, 21H, PCH(C*H*$_3$)$_2$), 1.23 (dd, $^3J_{HH}$ = 7 Hz, $^3J_{HP}$ = 17 Hz, PCH(C*H*$_3$)$_2$). Solubility constraints prevent us from acquiring the $^{13}C\{^1H\}$ NMR spectrum (Figure S15.). Ti=CH_2 was assigned at δ 290.3 by $^{13}C\{^1H\}$ NMR of **5-^{13}C**. $^{31}P\{^1H\}$ NMR (162 MHz, benzene-d_6, 300 K) δ 33.08 (d, $^2J_{PP}$ = 45 Hz, PNP), 22.50 (d, $^2J_{PP}$ = 45 Hz, PNP). Anal. Calcd. for $C_{45}H_{71}NOP_2Ti$: C, 71.89; H, 9.52; N, 1.86. Found: C, 71.39; H, 9.12; N, 1.80.

Synthesis of [(PNP)Ti(CH_3)$_2$(OTf)] (6)

To a green suspension of **1** (200 mg, 395 μmol) in hexane (10 mL) was added [$FeCp_2$][OTf] (167 mg, 498 μmol) in hexane (5 mL) at −35 °C. The mixture was vigorously stirred at room temperature for intermittent periods of 5 min, constantly placing the vial back in the freezer (−35 °C). After 5 periods of stirring in hexane, the reaction mixture changed color to a purple suspension/solution and then cold toluene (5 mL, –35 °C) was added. The mixture was stirred at room temperature for intermittent periods of 5 min again, placing the vial back in the freezer (−35 °C). After 5 periods of stirring in toluene/hexane, the reaction mixture was placed in the freezer (−35 °C) for 18 h and then the reaction mixture was filtered quickly through a medium porosity glass frit. The purple solid on the glass frit was extracted with cold toluene (10 mL, −35 °C). The combined purple filtrate was evaporated to dryness under reduced pressure. The residue was washed with cold pentane (5 mL, –35 °C) to yield **6** as purple solid (248 mg, 378 μmol calculated as **6**, 96% crude yield). ^{1}H NMR spectrum always shows some residual $FeCp_2$ and **7** (**6** : **7** : $FeCp_2$ = 1 : 0.13 : 0.06). ^{19}F{^{1}H} NMR spectra also shows some formation of **7** along with some unidentified impurities. Purple crystals of **6** for X-ray analysis were grown from concentrated pentane solution at −35 °C.

Selected data of **6**: ^{1}H NMR (400 MHz, benzene-d_6, 300 K): δ 6.89 (s, 2H, Ar-H), 6.81 (s, 4H, Ar-H), 3.34 (m, 2H, PC*H*(CH_3)$_2$), 2.13 (m, 2H, PC*H*(CH_3)$_2$) 2.07 (s, 6H, Ar-C*H*$_3$), 1.77 (t, $^{3}J_{HP}$ = 5 Hz, Ti-C*H*$_3$), 1.37 (dd, $^{3}J_{HH}$ = 7 Hz, $^{3}J_{HP}$ = 15 Hz, 6H, PCH(C*H*$_3$)$_2$), 1.18 (dd, $^{3}J_{HH}$ = 7 Hz, $^{3}J_{HP}$ = 16 Hz, 6H, PCH(C*H*$_3$)$_2$), 1.00 (dd, $^{3}J_{HH}$ = 8 Hz, $^{3}J_{HP}$ = 15 Hz, 6H, PCH(C*H*$_3$)$_2$), 0.87 (dd, $^{3}J_{HH}$ = 6 Hz, $^{3}J_{HP}$ = 17 Hz, 6H, PCH(C*H*$_3$)$_2$). ^{13}C{^{1}H} NMR (126 MHz, benzene-d_6, 300 K) δ.159.3 (PNP-Ar), 133.0 (PNP-Ar), 131.9 (PNP-Ar), 131.3 (PNP-Ar), 128.6 (PNP-Ar), 125.7 (PNP-Ar), 122.7 (PNP-Ar), 118.1 (PNP-Ar), 85.2 (t, $^{3}J_{CP}$ = 11 Hz, Ti-*C*H$_3$), 25.6 (P*C*H(CH_3)$_2$), 22.67 (P*C*H(CH_3)$_2$), 20.7 (Ar-*C*H$_3$), 19.6 (PCH(*C*H$_3$)$_2$), 19.3 (PCH(*C*H$_3$)$_2$), 19.1 (PCH(*C*H$_3$)$_2$), 17.3 (PCH(*C*H$_3$)$_2$).

Overlapping of the ^{13}C NMR spectrum prevents us from measuring some ^{13}C signals of CF_3. $^{31}P\{^1H\}$ NMR (162 MHz, benzene-d_6, 300 K) δ 29.52 (s, PNP). $^{19}F\{^1H\}$ NMR (282 MHz, benzene-d_6, 300 K) δ −77.02 (s, OTf).

Formation of [(PNP)Ti(=CH_2)(OTf)] (7)

In a J-Young valve NMR tube, a purple suspension of **6** (20.0 mg, 30.5 μmol) in benzene-d_6 (0.5 mL) was stored at room temperature in the absence of light. After 18 h, the color of the NMR sample changed to reddish brown, and formation of **7** (~ 70% conversion) and CH_4 was observed by ^1H NMR, $^{19}F\{^1H\}$ NMR and $^{31}P\{^1H\}$ NMR spectroscopy. The NMR sample then was photoirradiated with Xe-lamp at room temperature for 2 h. ^1H NMR spectrum (Figure S25.) showed formation of ethylene and unidentified paramagnetic species.

Selected data of **7**: ^1H NMR (400 MHz, benzene-d_6, 300 K): δ 11.58 (s, 2H, Ti=CH_2), 7.16 – 6.70 (m, 6H, Ar-H), 2.33 (m, 1H, PCH(CH_3)$_2$), 2.13 (s, 3H, Ar-CH_3), 2.06 (s, 3H, Ar-CH_3), 2.20 – 2.05 (m, 2H, PCH(CH_3)$_2$), 1.55 – 0.70 (m, 24H, PCH(CH_3)$_2$). $^{31}P\{^1H\}$ NMR (162 MHz, benzene-d_6, 300 K) δ 34.86 (d, $^2J_{PP}$ = 59 Hz, PNP), 25.16 (d, $^2J_{PP}$ = 59 Hz, PNP). $^{19}F\{^1H\}$ NMR (282 MHz, benzene-d_6, 300 K) δ −76.61 (s, OTf).

Synthesis of [(PNP)Ti($^{13}CH_3$)$_2$] (1-^{13}C)

To a Et_2O suspension (15 mL) of magnesium turnings (231 mg, 9.55 mmol) in a 100 mL J-Young valve tube was added $^{13}CH_3I$ (0.40 mL, 6.41 mmol) via a syringe at room temperature, resulting in an increase in temperature. After stirring for 18 h in the absence of light, the gray supernatant solution was filtered through glass wool in a pipette. The colorless filtrate of $H_3{}^{13}CMgI$ solution was added into an individually prepared (PNP)$TiCl_2$ suspension ($TiCl_3(THF)_3$, 850 mg, 2.64 mmol; Li(PNP), 1.00 g, 2.30 mmol) in toluene (30 mL) at –35 °C. To the greenish reaction mixture was added 1,4-dioxane (1.0 mL) via a syringe. After stirring for 2 h at room temperature, the reaction mixture

was evaporated to dryness under reduced pressure. The gray residue was extracted into toluene (150 mL) and the suspension was filtered through a medium porosity glass frit containing Celite. The Celite was washed twice with toluene (2 × 20 mL) to extract the residue. The green filtrate was evaporated to dryness and the residue was washed twice with pentane (2 × 5 mL) to give **1-^{13}C** as green solid (286 mg, 562 μmol, 25% yield). Paramagnetic broadening prevents us from observing any significant differences of the ^{1}H NMR spectrum to that of **1**.

Synthesis and NMR Studies of [(PNP)Ti($^{13}CH_3$)$_2$(TEMPO)] (2-^{13}C) and [(PNP)Ti($^{13}CH_3$){ONC$_5$H$_6$(CH$_3$)$_3$(CH$_2$)}] (4-^{13}C)

In a J-Young valve NMR tube, a green suspension of **1-^{13}C** (20.1 mg, 39.5 μmol) in benzene-d_6 (0.5 mL) was treated with TEMPO (6.5 mg, 41.6 μmol) at room temperature. After shaking the NMR sample for 10 min, the color of the NMR sample changed to orange and formation of **2-^{13}C** was observed by ^{1}H NMR, ^{13}C{^{1}H} NMR, ^{31}P{^{1}H} NMR, ^{1}H-^{13}C HMQC and ^{1}H-^{13}C HMBC spectral data. The NMR sample was heated at 60 °C for 6 h in the absence of light and then ^{1}H NMR, ^{13}C{^{1}H} NMR, ^{31}P{^{1}H} NMR and ^{1}H-^{13}C HMQC spectra were measured to show formation of **4-^{13}C** and $^{13}CH_4$.

Selected data of **2-^{13}C**: ^{13}C{^{1}H} NMR (126 MHz, benzene-d_6, 300 K): δ 60.4 (br, Ti*C*H$_3$). Selected ^{1}H-^{13}C HMQC NMR chemical shifts (500 MHz, benzene-d_6, 300 K): δ ^{1}H (δ ^{13}C) 2.07 (60.4). ^{1}H-^{13}C HMBC NMR chemical shifts (500 MHz, benzene-d_6, 300 K): δ ^{1}H (δ ^{13}C) 2.07 (60.4, $^{1}J_{CH}$ = 121 Hz). The ^{31}P{^{1}H} NMR spectrum shows more broaden signal than that of non-labeled **2**.

Selected data of **4-^{13}C**: ^{13}C{^{1}H} NMR (126 MHz, benzene-d_6, 300 K): δ 30.0 (s, Ti*C*H$_3$). Selected ^{1}H-^{13}C HMQC NMR chemical shifts (500 MHz, benzene-d_6, 300 K): δ ^{1}H (δ ^{13}C) 2.61 (30.0). The ^{31}P{^{1}H} NMR spectrum shows more broaden signal than non-labeled **2**. The ^{31}P{^{1}H} NMR spectrum shows similar signals to those of non-labeled **2** due to its too small J_{CP} coupling.

Synthesis and NMR Studies of [(PNP)Ti($^{13}CH_3$)$_2$(OMes*)] (3-^{13}C) and [(PNP)Ti(=$^{13}CH_2$)(OMes*)] (5-^{13}C)

In a J-Young valve NMR tube, a green suspension of **1-^{13}C** (19.9 mg, 39.1 μmol) in benzene-d_6 (0.5 mL) was treated with •OMes* (11.1 mg, 42.3 μmol) at room temperature. After shaking the NMR sample for 10 min, the color of the NMR sample gradually changed from unreacted blue-green to dark brown and formation of **3-^{13}C** and small amount of **5-^{13}C** was observed by ^{1}H NMR, ^{13}C{^{1}H} NMR, ^{31}P{^{1}H} NMR, ^{1}H-^{13}C HMQC and ^{1}H-^{13}C HMBC spectral data. ^{13}C-^{13}C EXSY spectrum of **3-^{13}C** was also measured to show exchanging of two inequivalent $^{13}CH_3$ groups in **3-^{13}C**. The NMR sample was heated at 70 °C for 6 h and formation of **5-^{13}C** and $^{13}CH_4$ was observed by ^{1}H NMR, ^{13}C{^{1}H} NMR, ^{31}P{^{1}H} NMR, and ^{1}H-^{13}C HMQC spectral data.

Selected data of **3-^{13}C**: ^{13}C{^{1}H} NMR (126 MHz, benzene-d_6, 300 K): δ 82.9 (d, J_{CP} = 12 Hz, Ti*C*H$_3$), 56.4 (d, J_{CP} = 10 Hz, Ti*C*H$_3$). Selected ^{1}H-^{13}C HMQC NMR chemical shifts (500 MHz, benzene-d_6, 300 K): δ ^{1}H (δ ^{13}C) 2.05 (56.4) 1.70 (82.9). ^{1}H-^{13}C HMBC NMR chemical shifts (500 MHz, benzene-d_6, 300 K): δ ^{1}H (δ ^{13}C) 2.05 (82.9, $^1J_{CH}$ = 124 Hz), 1.70 (56.4, $^1J_{CH}$ = 124 Hz). ^{31}P{^{1}H} NMR (162 MHz, benzene-d_6, 300 K) δ 26.77 (d, $^2J_{CP}$ = 10 Hz, PNP), –8.21 (d, $^2J_{CP}$ = 12 Hz, PNP).

Selected data of **5-^{13}C**: ^{1}H NMR (400 MHz, benzene-d_6, 300 K): δ 14.20 (d, $^1J_{CH}$ = 125 Hz, Ti=^{13}C*H*$_2$). ^{13}C{^{1}H} NMR (126 MHz, benzene-d_6, 300 K, selected data): δ 290.3 (t, Ti=*C*H$_2$). Selected ^{1}H-^{13}C HMQC NMR chemical shifts (500 MHz, benzene-d_6, 300 K): δ ^{1}H (δ ^{13}C) 14.20 (290.3). ^{31}P{^{1}H} NMR (162 MHz, benzene-d_6, 300 K) δ 37.20 (dd, $^2J_{PP}$ = 59 Hz, $^2J_{CP}$ = 11 Hz, PNP), 25.75 (dd, $^2J_{PP}$ = 59 Hz, $^2J_{CP}$ = 11 Hz, PNP).

Synthesis of [(PNP)Ti($^{13}CH_3$)$_2$(OTf)] (6-^{13}C)

The same procedure as used for **6** was followed. Addition of [$FeCp_2$][OTf] (66.1 mg, 239 μmol) in hexane (5 mL) to a hexane suspension (10 mL) of **1-^{13}C** (85.0 mg, 254 μmol) afforded **6-^{13}C** (106 mg, 161 μmol calculated as **6-^{13}C**, 67% crude yield) as purple solid. The ^{1}H NMR spectrum of **6-^{13}C** shows some residual $FeCp_2$ and **7-^{13}C**.

Selected data of **6-^{13}C**: ^{1}H NMR (400 MHz, benzene-d_6, 300 K): δ 1.77 (dt, $^3J_{HP}$ = 5 Hz, $^1J_{CH}$ = 125 Hz, Ti-$^{13}CH_3$). ^{13}C{^{1}H} NMR spectrum shows same signal of Ti-CH_3 with that of non-labeled **6**, but much stronger intensity. Selected ^{1}H-^{13}C HMQC NMR chemical shifts (500 MHz, benzene-d_6, 300 K): δ ^{1}H (δ ^{13}C) 1.77 (85.2). ^{1}H-^{13}C HMBC NMR chemical shifts (500 MHz, benzene-d_6, 300 K): δ ^{1}H (δ ^{13}C) 1.77 (85.2, $^1J_{CH}$ = 125 Hz). ^{31}P{^{1}H} NMR (162 MHz, benzene-d_6, 300 K) δ 29.52 (d, $^2J_{CP}$ = 11 Hz, PNP).

Formation of [(PNP)Ti(=$^{13}CH_2$)(OTf)] (7-^{13}C)

In a J-Young valve NMR tube, a purple suspension of **6-^{13}C** (18.1 mg, 27.5 μmol) in benzene-d_6 (0.5 mL) was stored at room temperature in the absence of light. After 20 h, the color of the NMR sample changed to reddish brown, and formation of **7-^{13}C** and $^{13}CH_4$ was observed by ^{1}H NMR, ^{13}C{^{1}H} NMR, and ^{31}P{^{1}H} NMR spectroscopy. The NMR sample was then photoirradiated with a Xe-lamp at room temperature for 3 h. The ^{1}H NMR and ^{13}C{^{1}H} spectra (Figure S50. and S51.) showed formation of $^{13}C_2H_4$ (^{1}H: 5.25, ^{13}C: 122.9 ppm, $^1J_{CH}$ = 154 Hz) and unidentified paramagnetic species.

Selected data of **7-^{13}C**: ^{1}H NMR (400 MHz, benzene-d_6, 300 K): δ 11.58 (d, $^1J_{CH}$ = 126 Hz, Ti=$^{13}CH_2$). ^{13}C{^{1}H} NMR (126 MHz, benzene-d_6, 300 K): δ. 295.9 (t, Ti=CH_2). Selected ^{1}H-^{13}C HMQC NMR chemical shifts (500 MHz, benzene-d_6, 300 K): δ ^{1}H (δ ^{13}C) 11.58 (295.9). ^{31}P{^{1}H} NMR (162 MHz, benzene-d_6, 300 K) δ 34.86 (dd, $^2J_{PP}$ = 59 Hz, $^2J_{CP}$ = 11 Hz, PNP), 25.16 (dd, $^2J_{PP}$ = 59 Hz, $^2J_{CP}$ = 11 Hz, PNP).

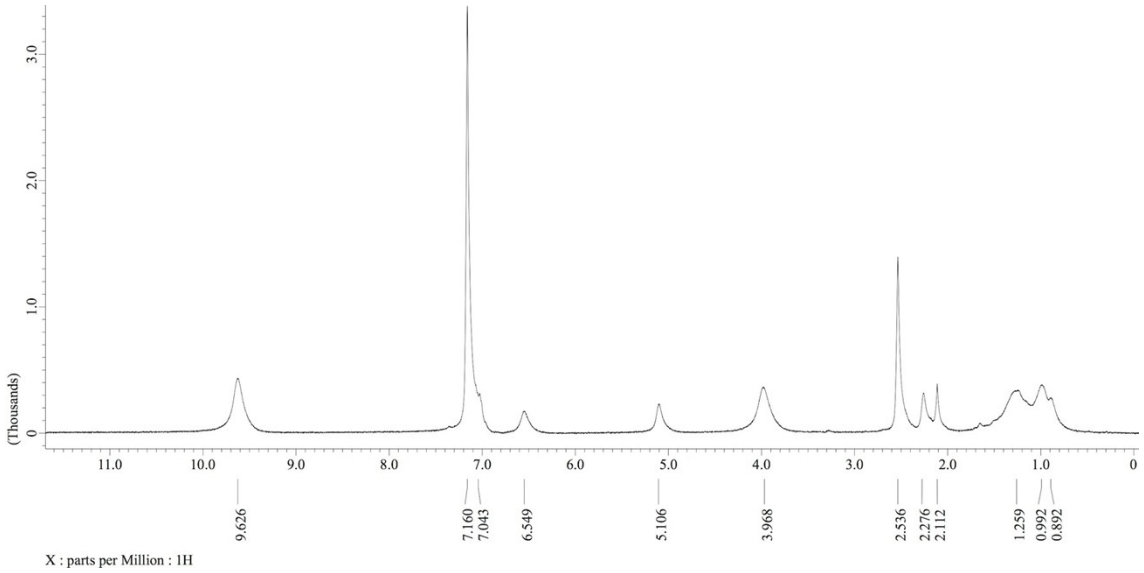

Figure S1. ^{1}H NMR spectrum of **1** (400 MHz, in benzene-d_6, at 300 K).

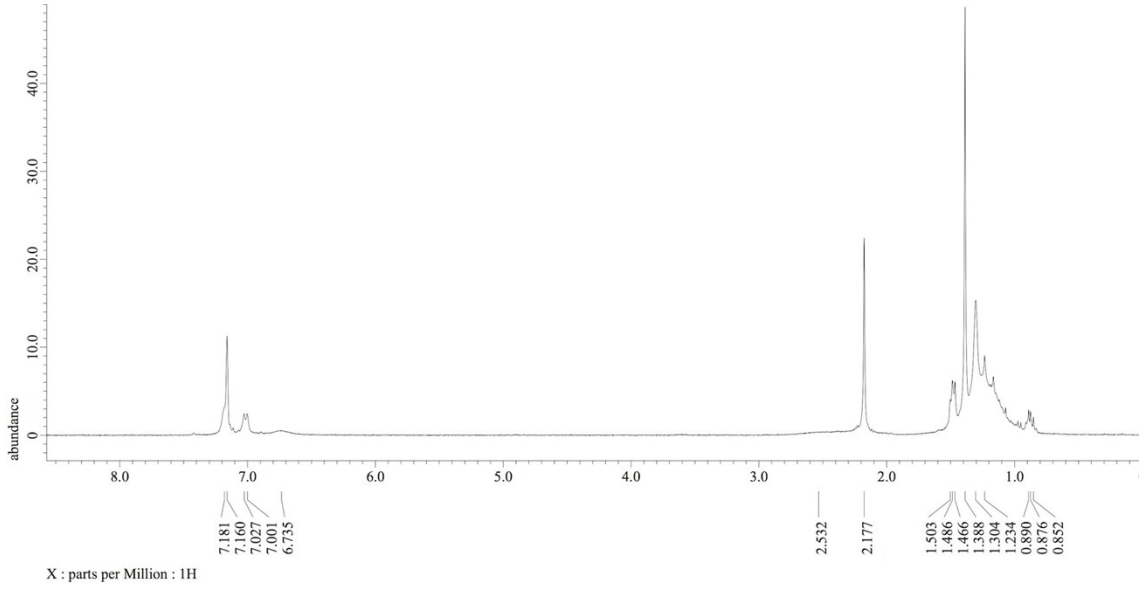

Figure S2. ^{1}H NMR spectrum of **2** (400 MHz, in benzene-d_6, at 300 K).

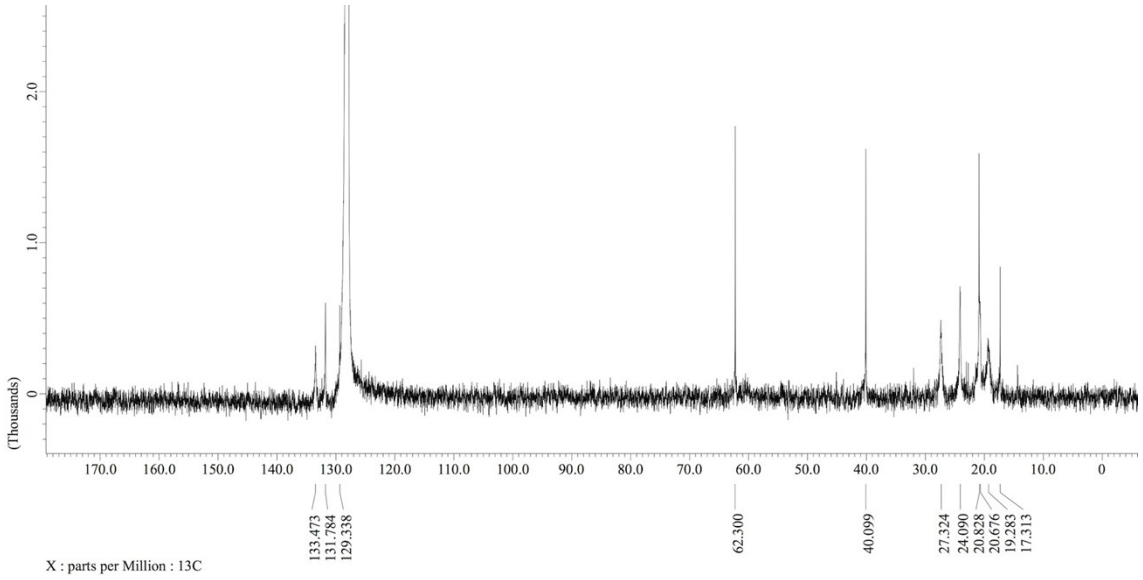

Figure S3. $^{13}C\{^{1}H\}$ NMR spectrum of **2** (126 MHz, in benzene-d_6, at 300 K).

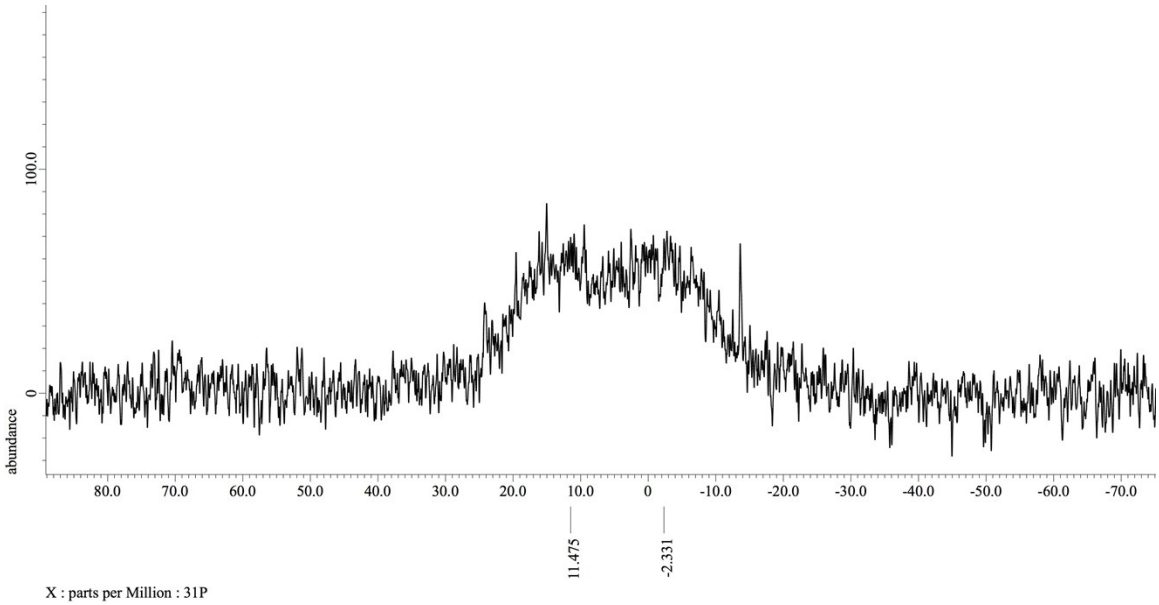

Figure S4. $^{31}P\{^{1}H\}$ NMR spectrum of **2** (162 MHz, in benzene-d_6, at 300 K).

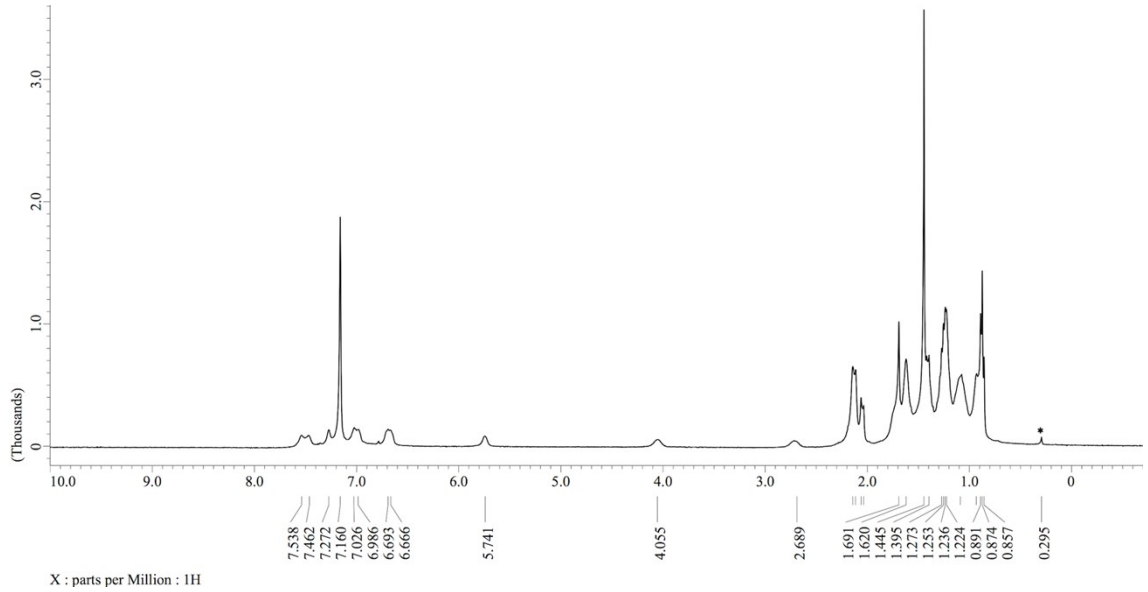

Figure S5. ^{1}H NMR spectrum of **3** (400 MHz, in benzene-d_6, at 300 K). *: grease

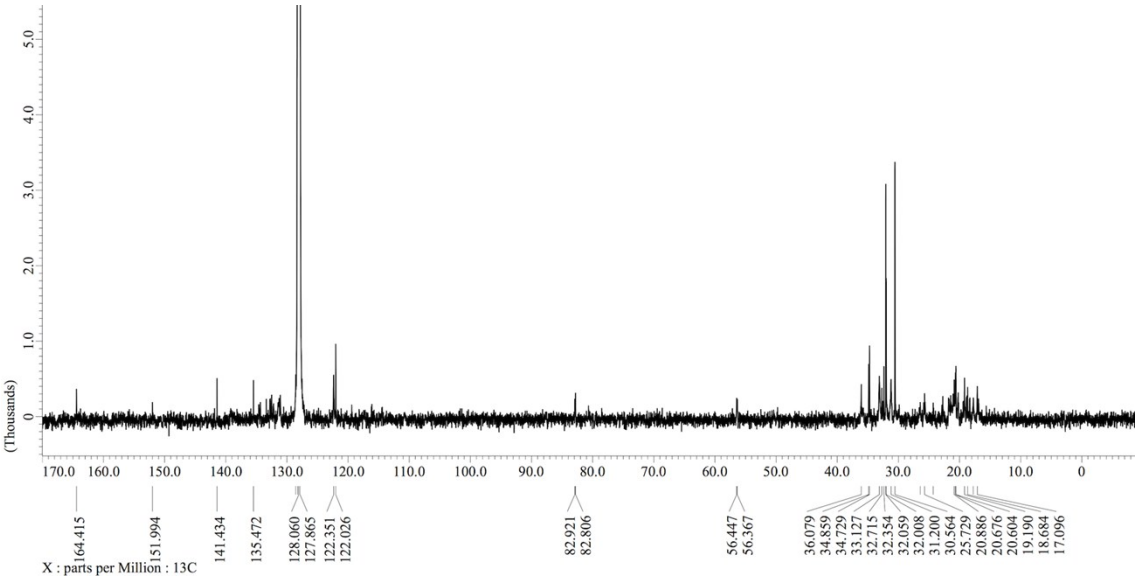

Figure S6. ^{13}C{^{1}H} NMR spectrum of **3** (126 MHz, in benzene-d_6, at 300 K).

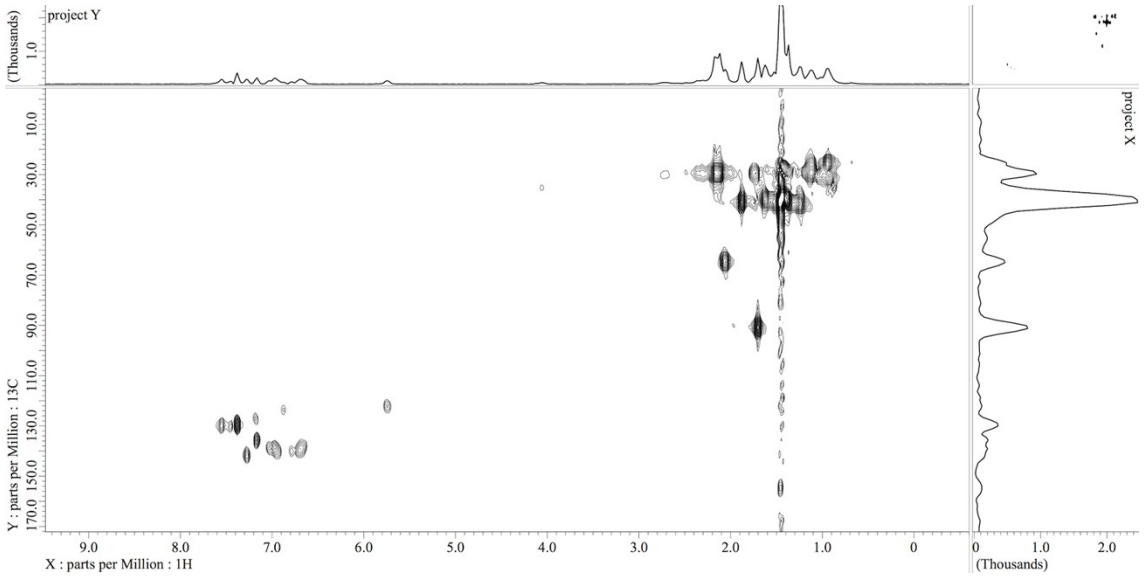

Figure S7. ^{1}H-^{13}C HMQC spectrum of **3** (500 MHz, in benzene-d_6, at 300 K).

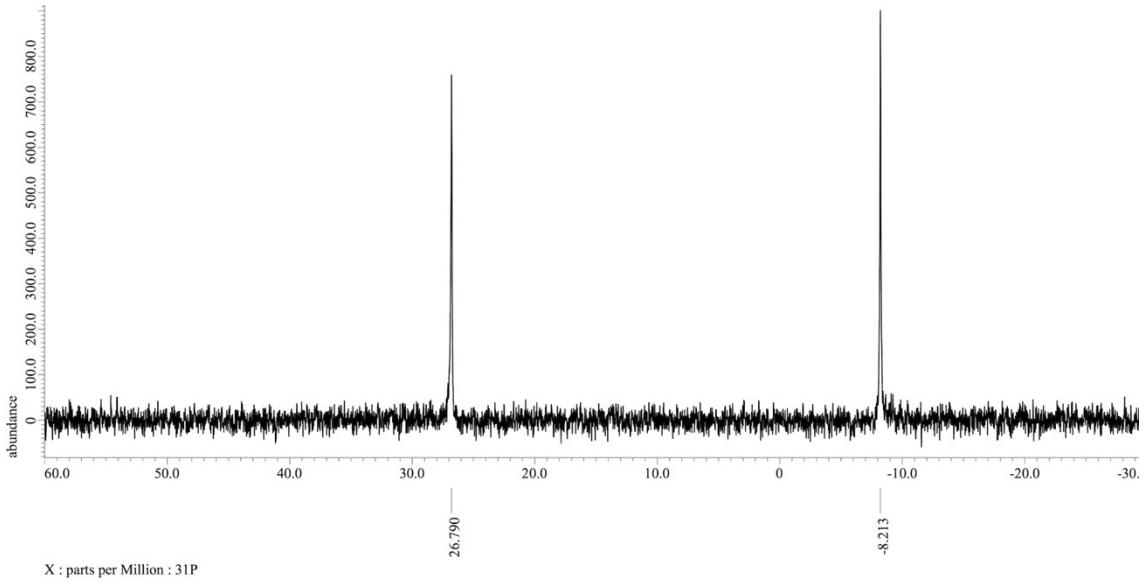

Figure S8. $^{31}P\{^{1}H\}$ NMR spectrum of **3** (162 MHz, in benzene-d_6, at 300 K).

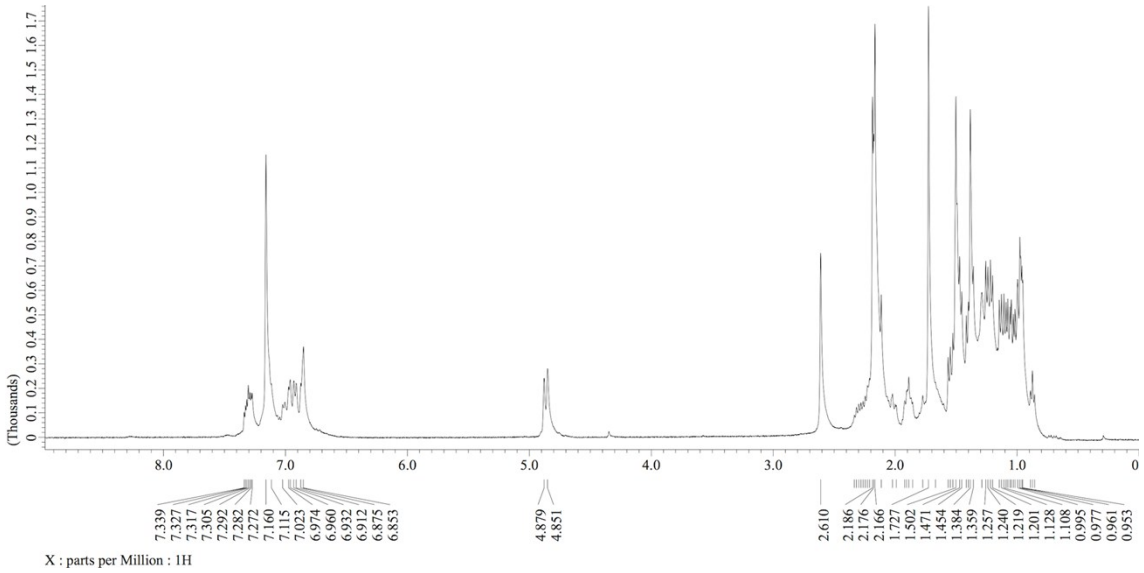

Figure S9. ^{1}H NMR spectrum of **4** (400 MHz, in benzene-d_6, at 300 K).

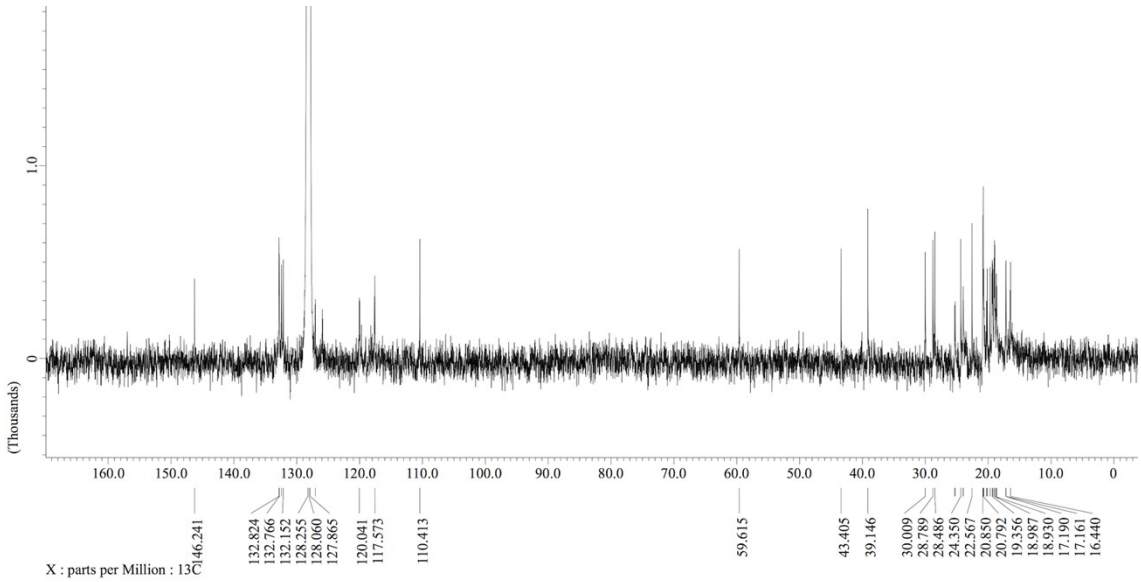

Figure S10. ^{13}C{^{1}H} NMR spectrum of **4** (126 MHz, in benzene-d_6, at 300 K).

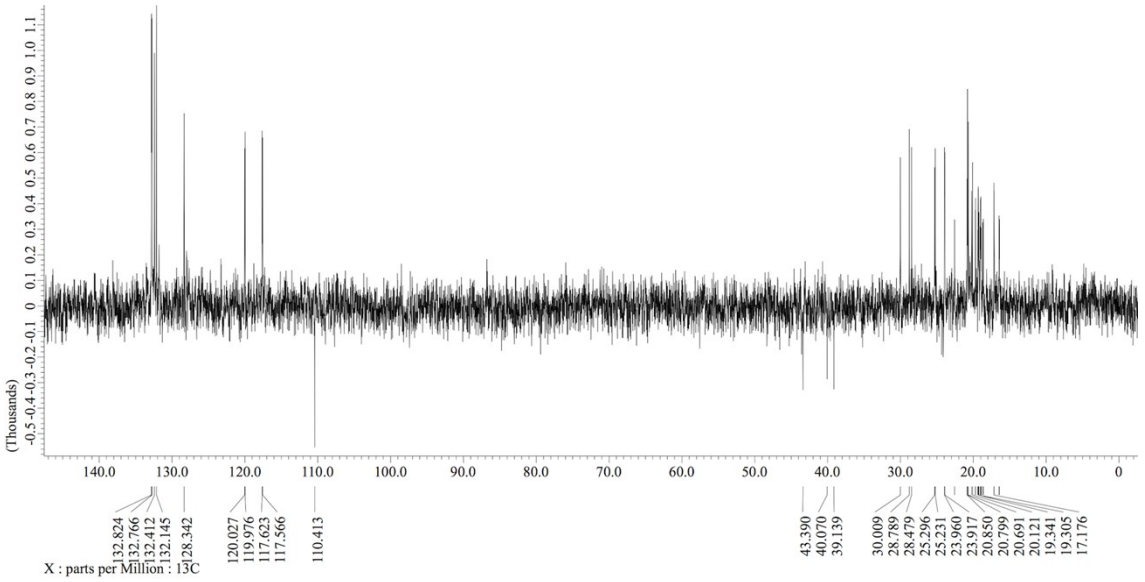

Figure S11. DEPT135° ^{13}C NMR spectrum of **4** (126 MHz, in benzene-d_6, at 300 K).

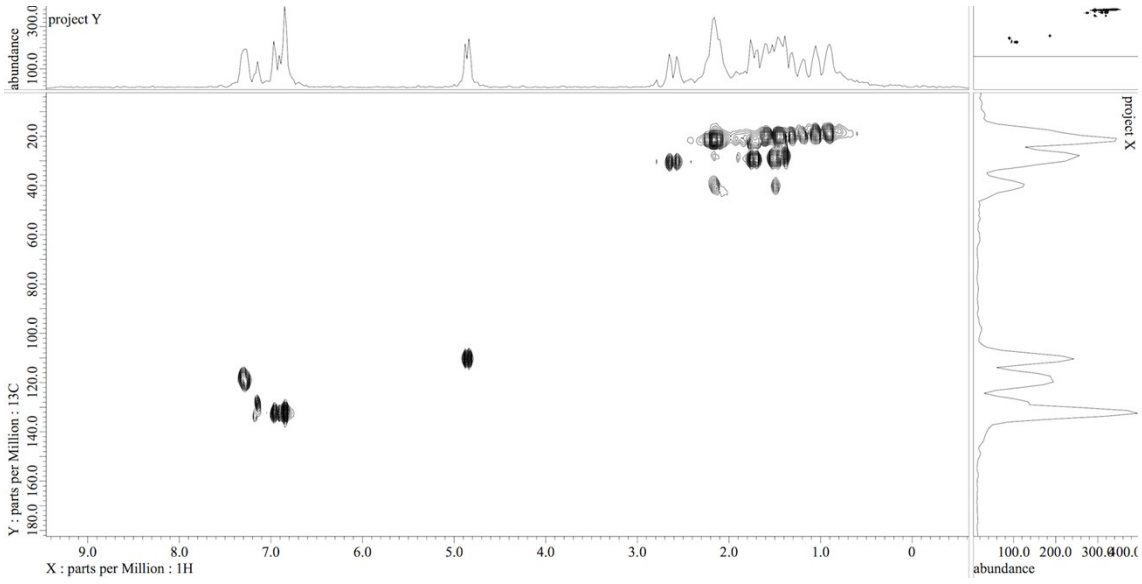

Figure S12. ^{1}H-^{13}C HMQC spectrum of **4** (500 MHz, in benzene-d_6, at 300 K).

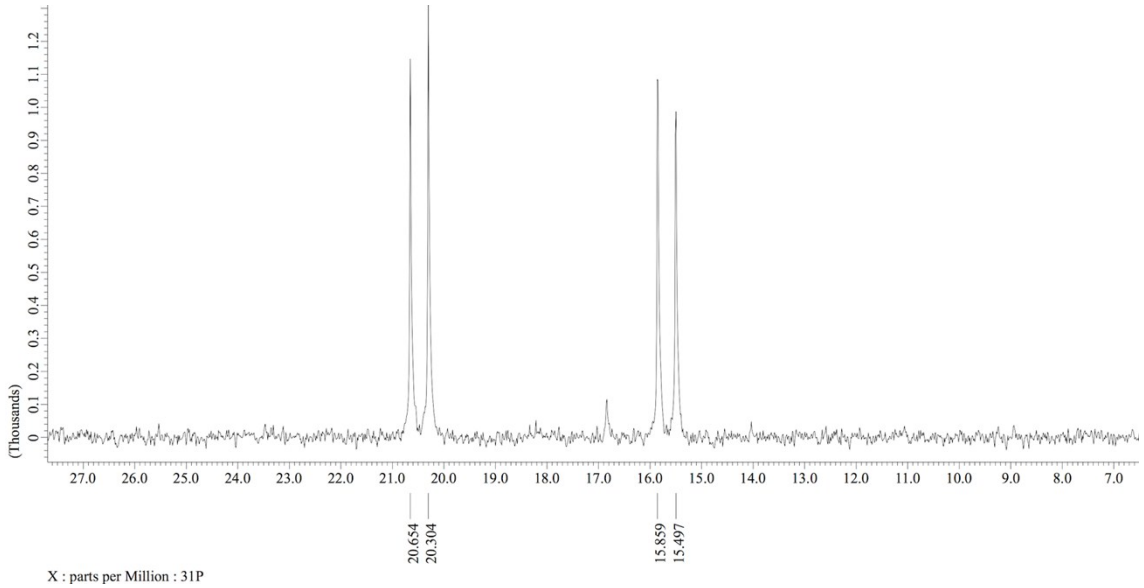

Figure S13. $^{31}P\{^{1}H\}$ NMR spectrum of **4** (162 MHz, in benzene-d_6, at 300 K).

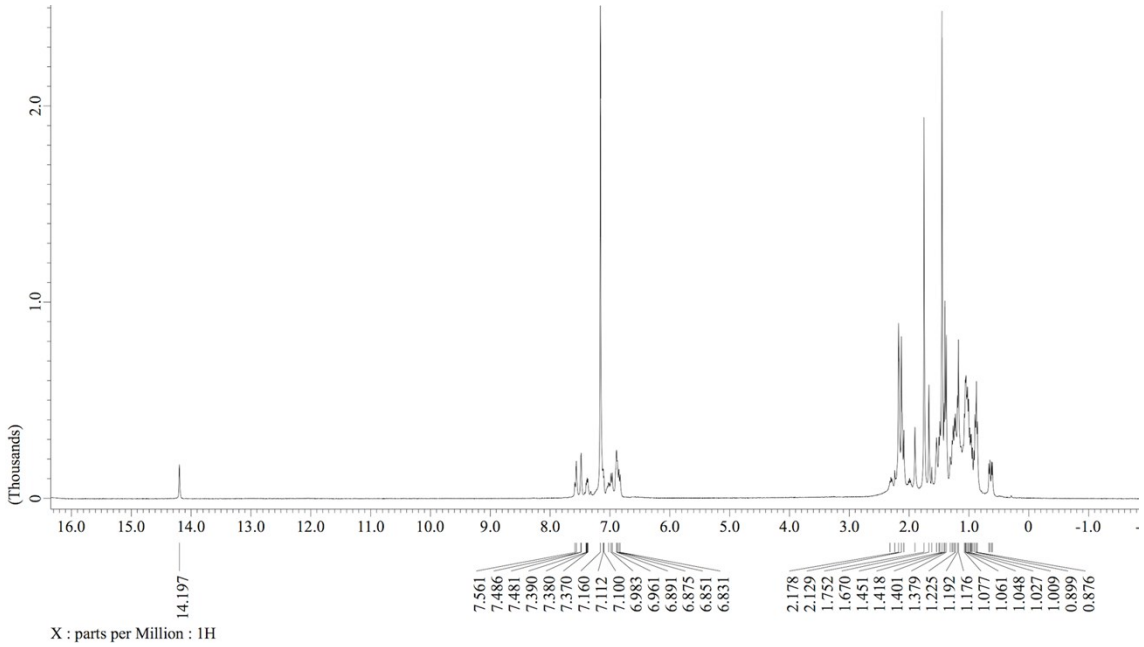

Figure S14. ^{1}H NMR spectrum of **5** (400 MHz, in benzene-d_6, at 300 K).

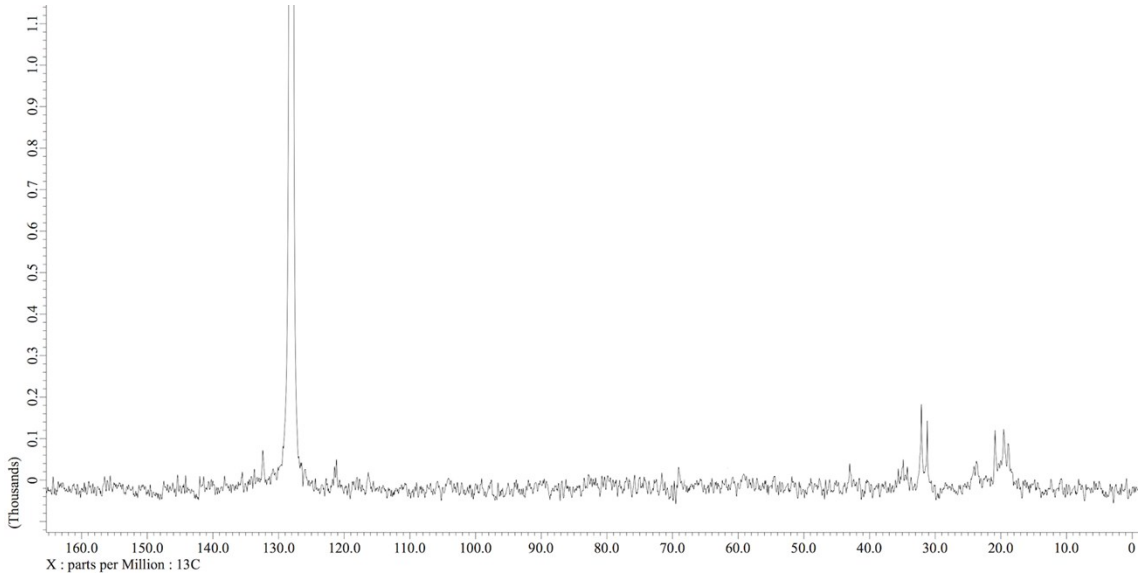

Figure S15. $^{13}C\{^{1}H\}$ NMR spectrum of **5** (126 MHz, in benzene-d_6, at 300 K).

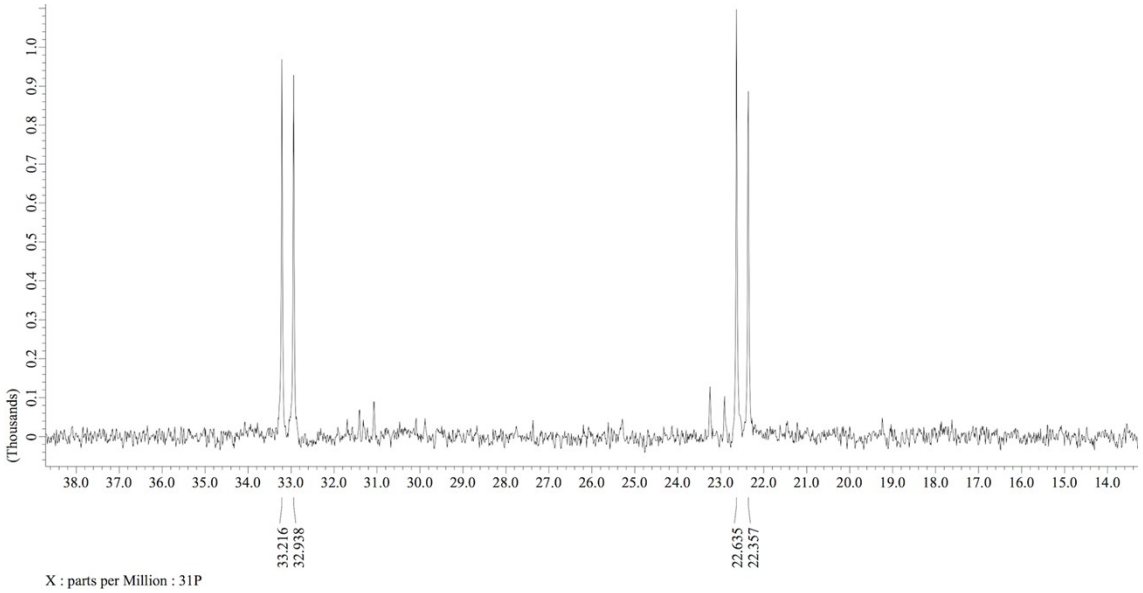

Figure S16. $^{31}P\{^{1}H\}$ NMR spectrum of **5** (162 MHz, in benzene-d_6, at 300 K).

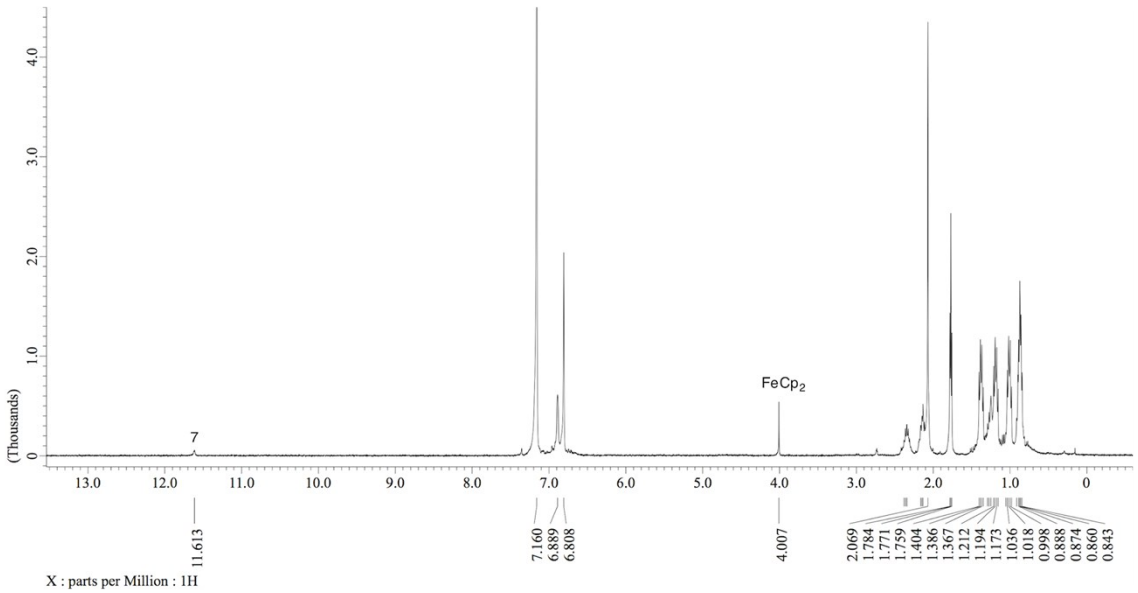

Figure S17. ^{1}H NMR spectrum of **6** (400 MHz, in benzene-d_6, at 300 K).

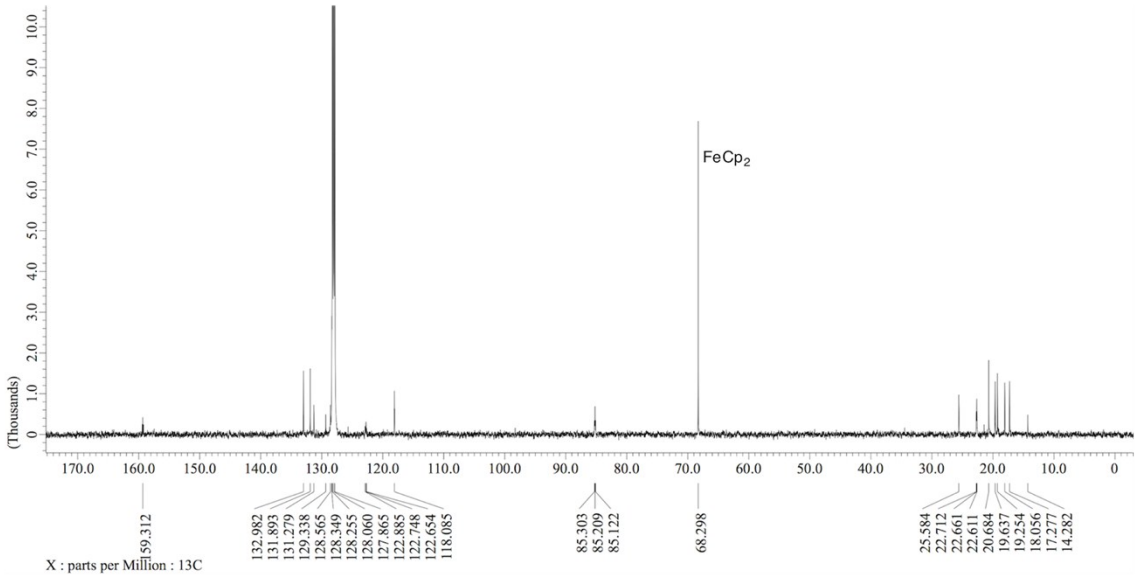

Figure S18. ^{13}C{^{1}H} NMR spectrum of **6** (126 MHz, in benzene-d_6, at 300 K).

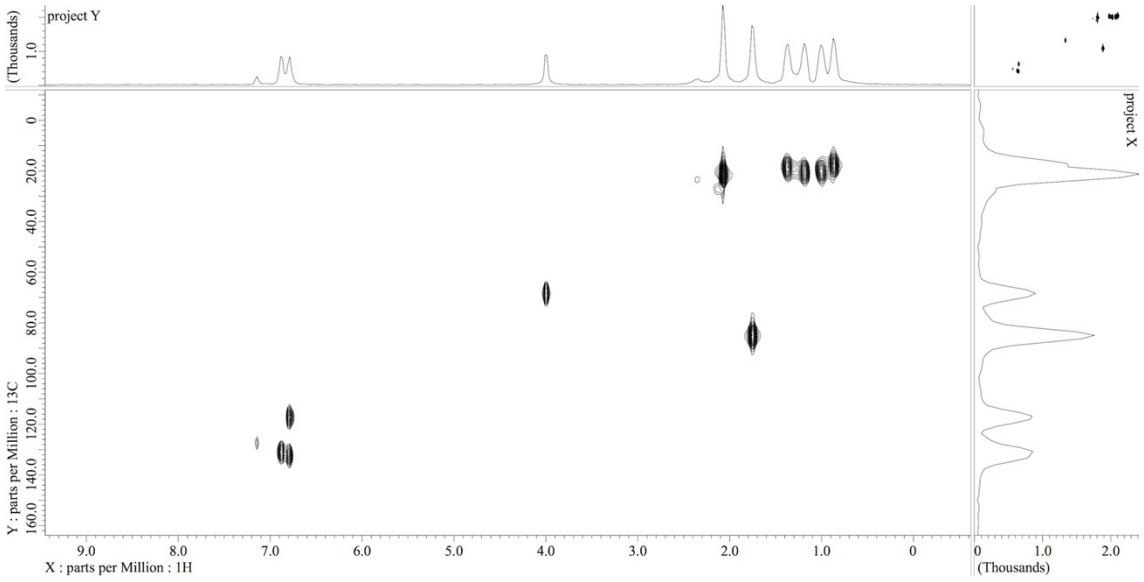

Figure S19. ^{1}H-^{13}C HMQC spectrum of **6** (500 MHz, in benzene-d_6, at 300 K).

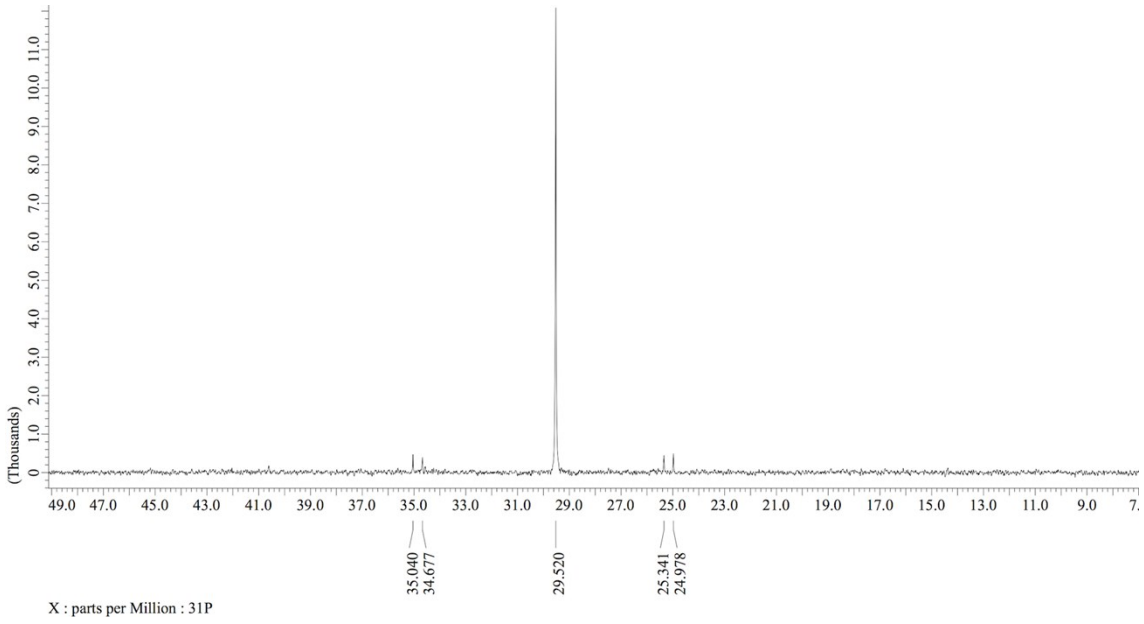

Figure S20. ^{31}P{^{1}H} NMR spectrum of **6** (162 MHz, in benzene-d_6, at 300 K).

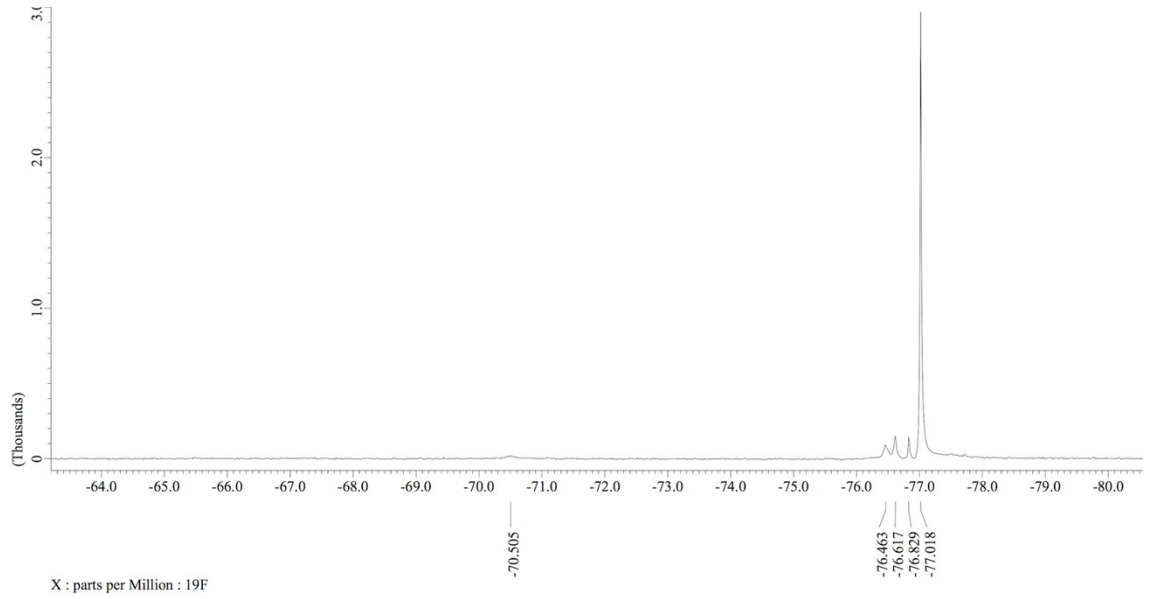

Figure S21. $^{19}F\{^{1}H\}$ NMR spectrum of **6** (282 MHz, in benzene-d_6, at 300 K).

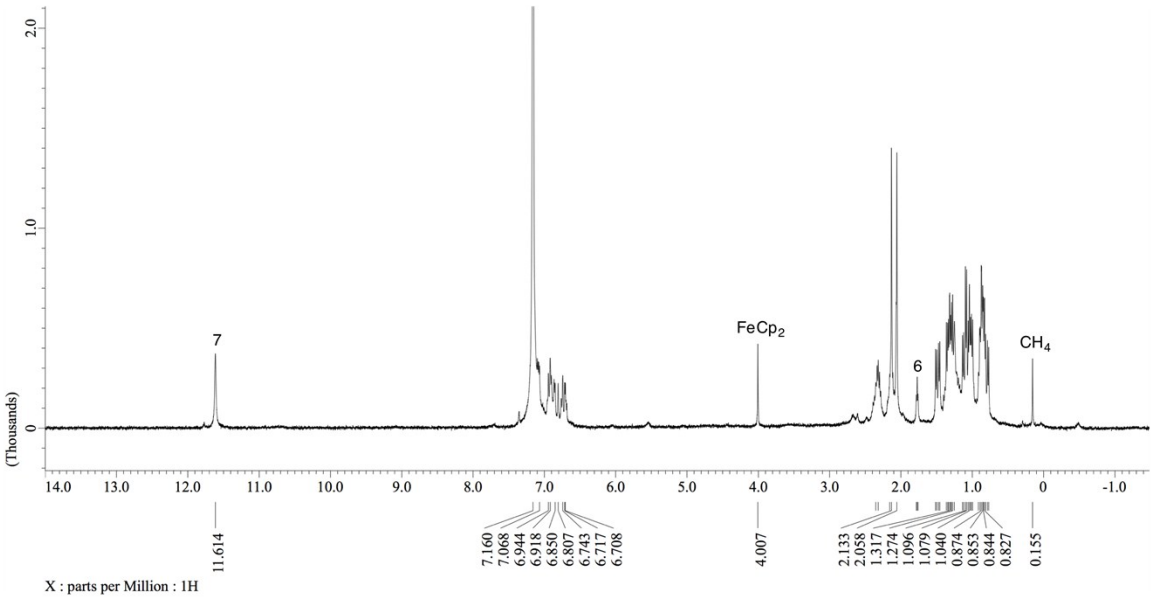

Figure S22. ^{1}H NMR spectrum of benzene-d_6 solution of **6** after 18 h at room temperature (400 MHz, in benzene-d_6, at 300 K).

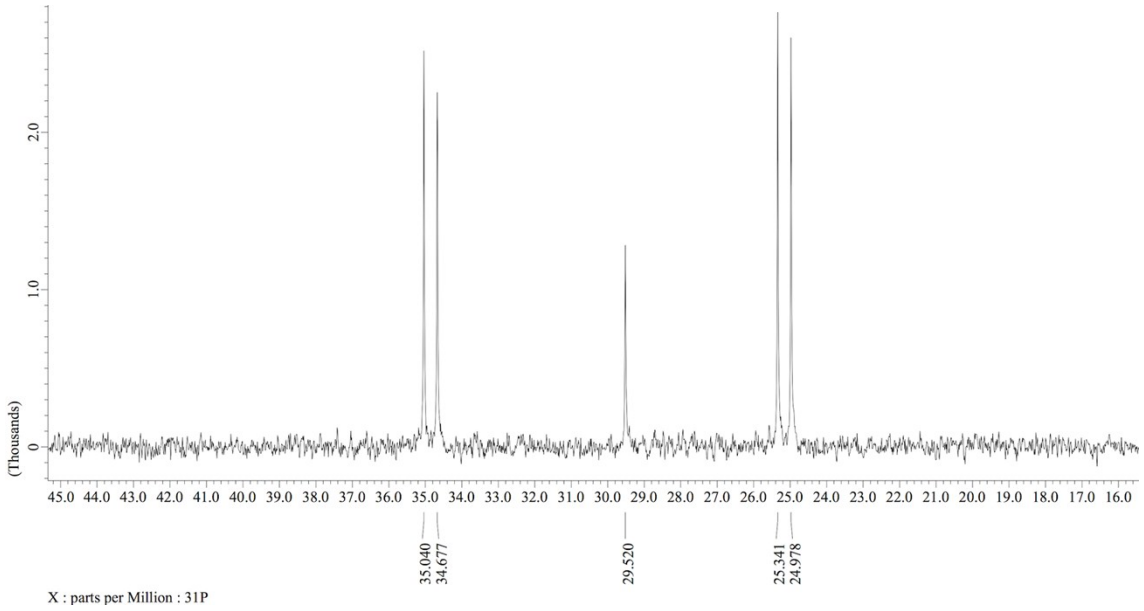

Figure S23. $^{31}P\{^{1}H\}$ NMR spectrum of benzene-d_6 solution of **6** after 18 h at room temperature (162 MHz, in benzene-d_6, at 300 K).

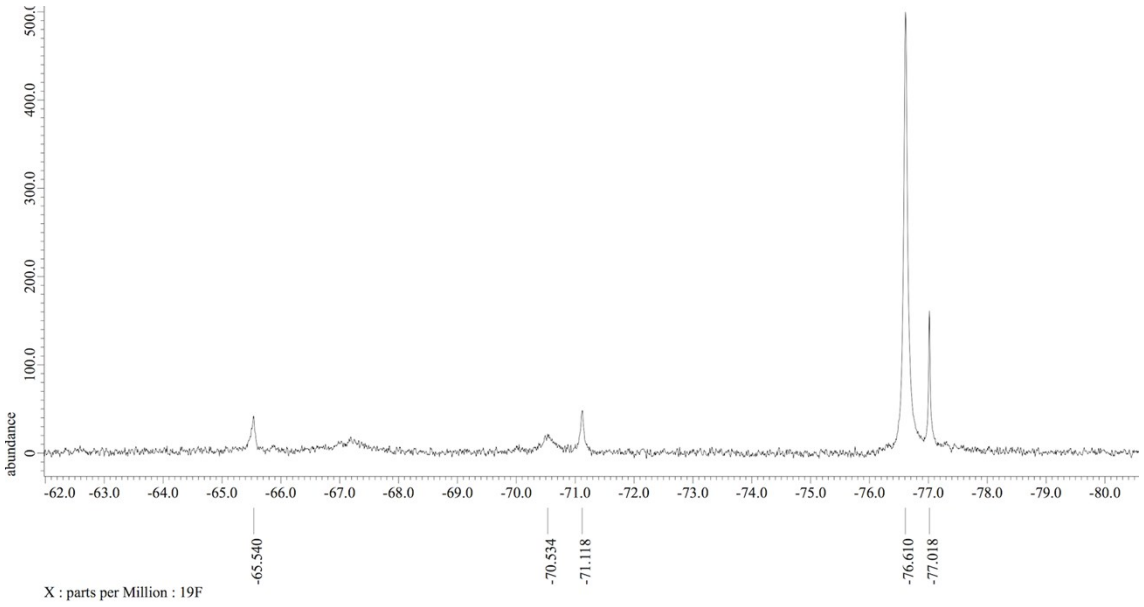

Figure S24. $^{19}F\{^{1}H\}$ NMR spectrum of benzene-d_6 solution of **6** after 18 h at room temperature (282 MHz, in benzene-d_6, at 300 K).

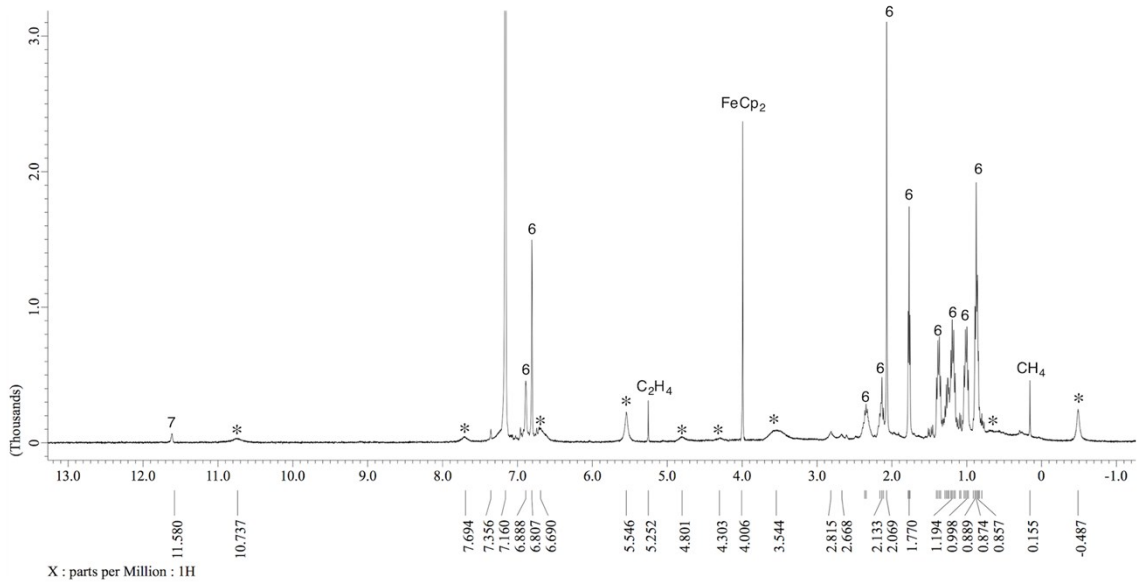

Figure S25. ^{1}H NMR spectrum of benzene-d_6 solution after photolysis of **7** (400 MHz, in benzene-d_6, at 300 K). *: unidentified species.

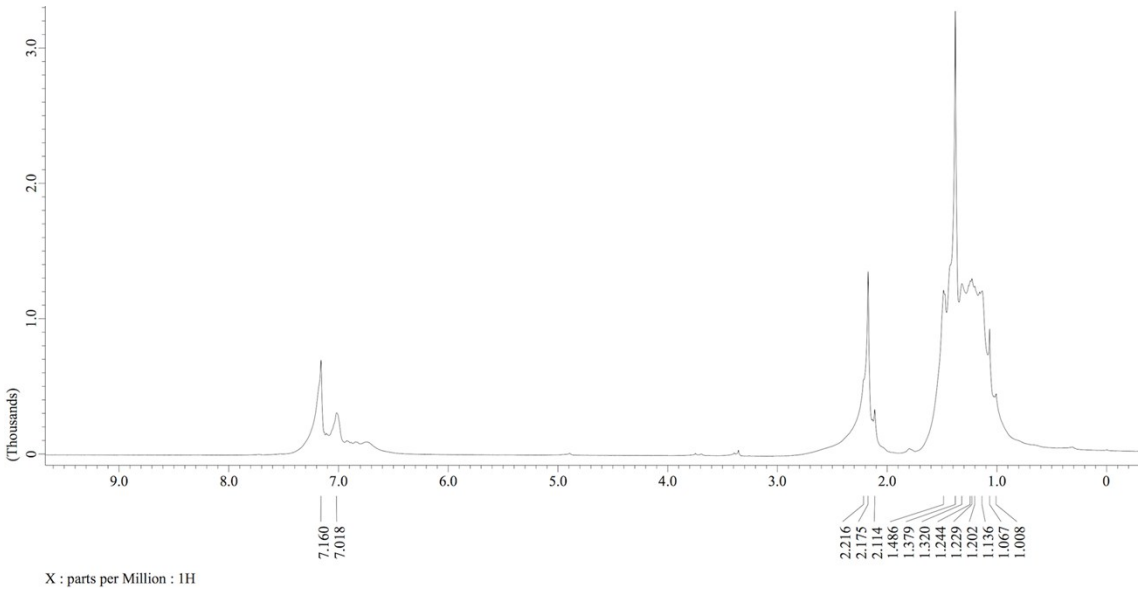

Figure S26. ^{1}H NMR spectrum of benzene-d_6 solution of **2-^{13}C** (400 MHz, in benzene-d_6, at 300 K).

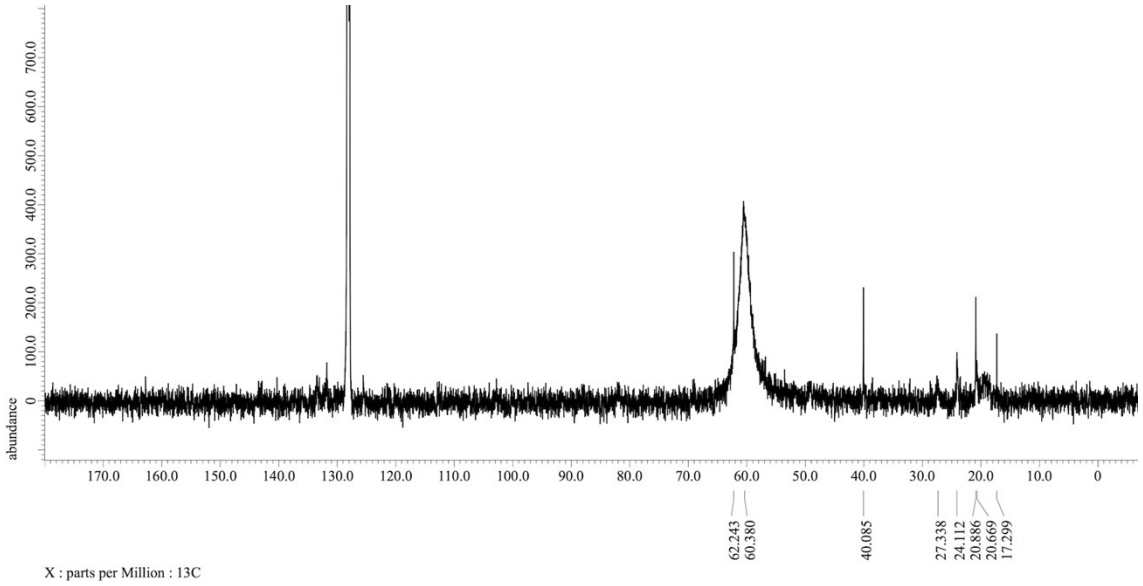

Figure S27. $^{13}C\{^{1}H\}$ NMR spectrum of **2-^{13}C** (126 MHz, in benzene-d_6, at 300 K).

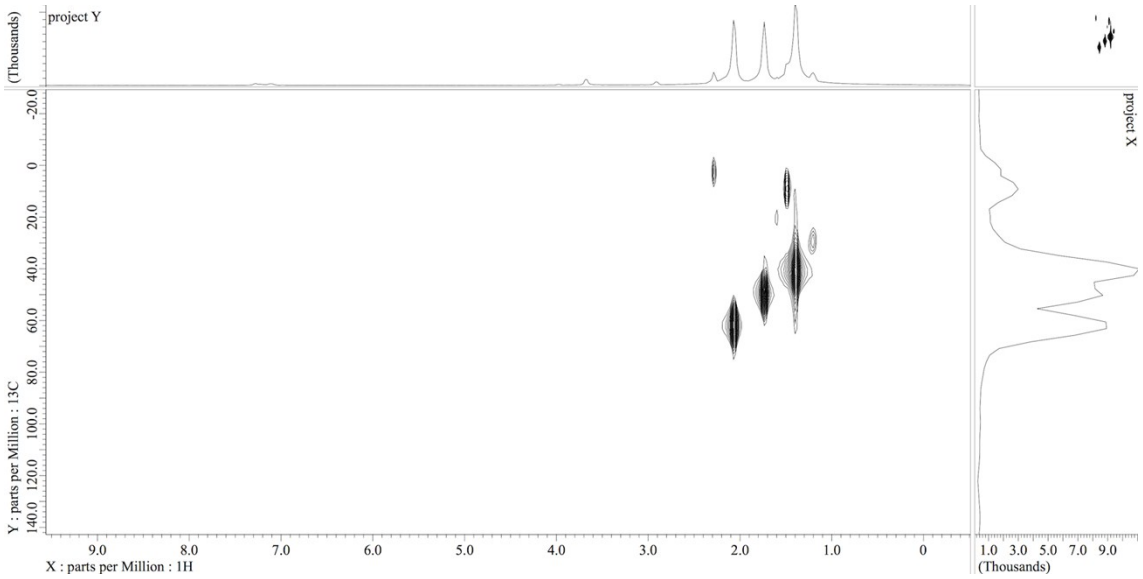

Figure S28. ^{1}H-^{13}C HMQC spectrum of **2-^{13}C** (500 MHz, in benzene-d_6, at 300 K).

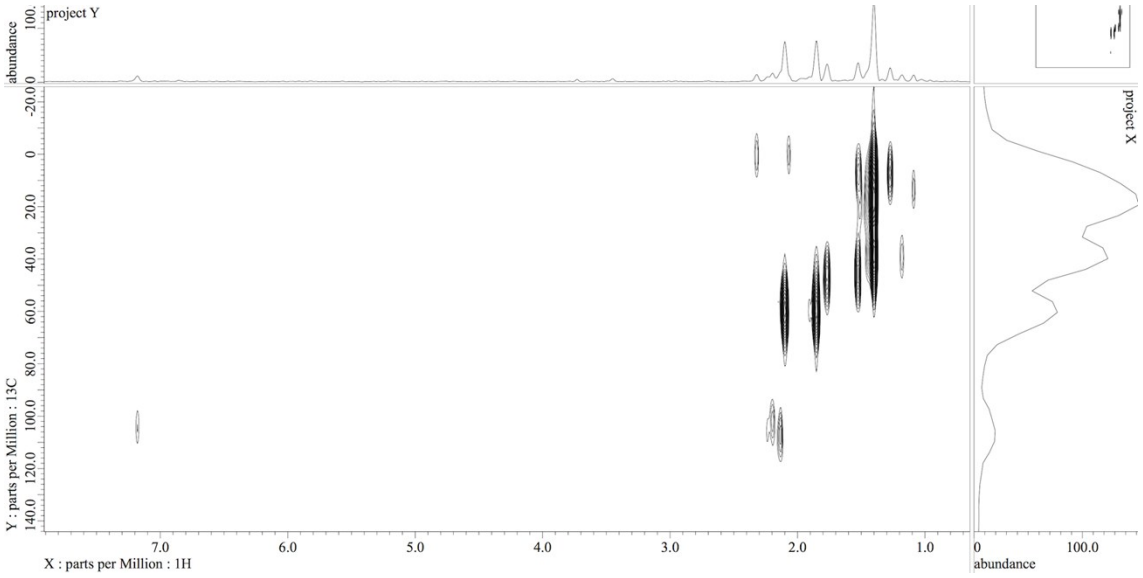

Figure S29. ^{1}H-^{13}C HMBC spectrum of **2-^{13}C** (500 MHz, in benzene-d_6, at 300 K).

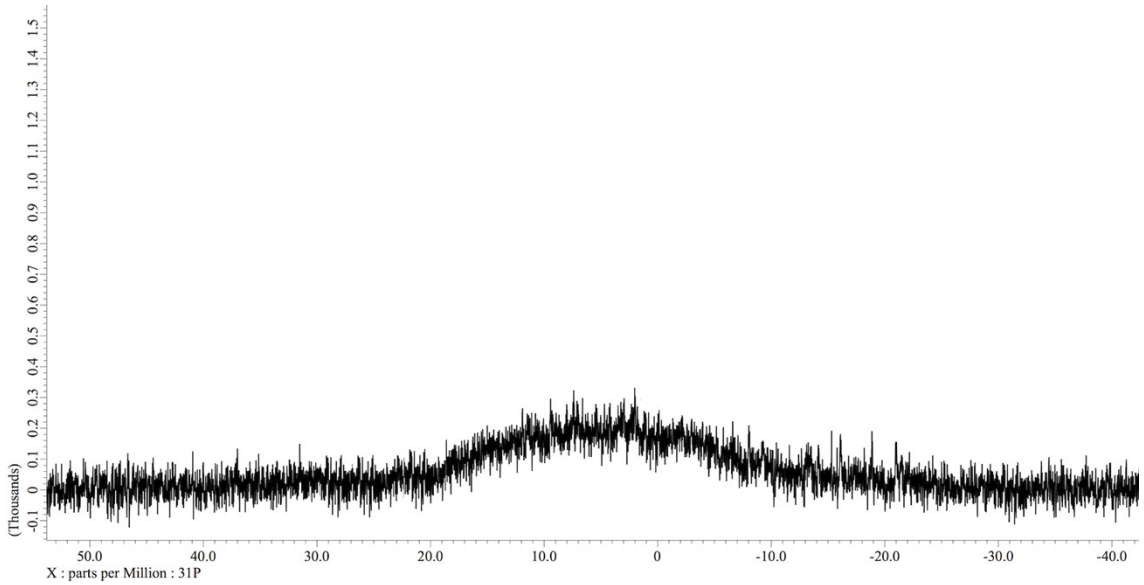

Figure S30. ^{31}P{^{1}H} NMR spectrum of **2-^{13}C** (162 MHz, in benzene-d_6, at 300 K).

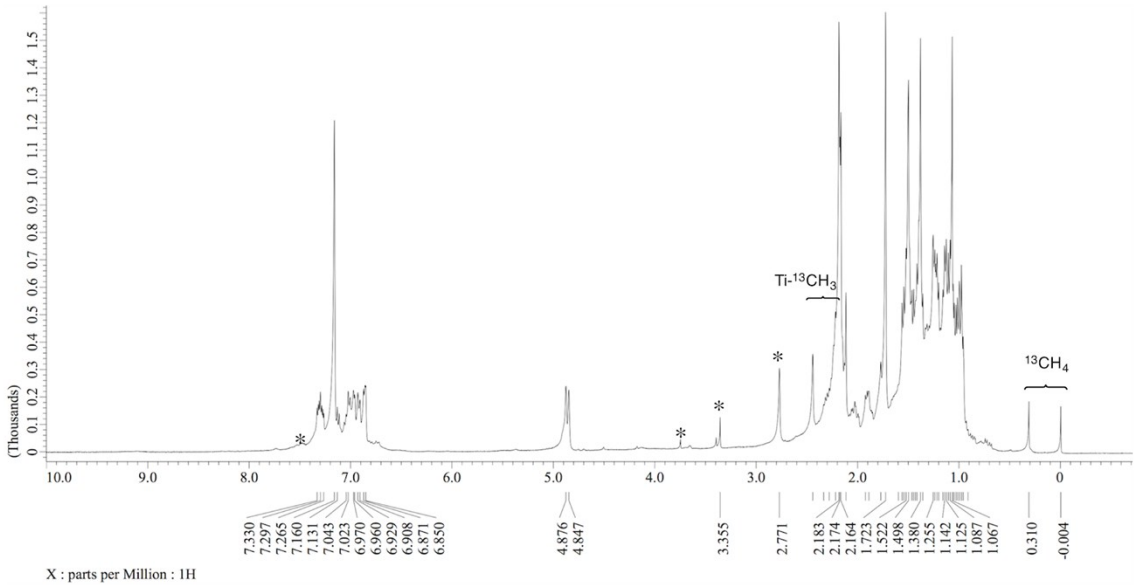

Figure S31. ^{1}H NMR spectrum of benzene-d_6 solution of **4-^{13}C** (400 MHz, in benzene-d_6, at 300 K). *: impurity.

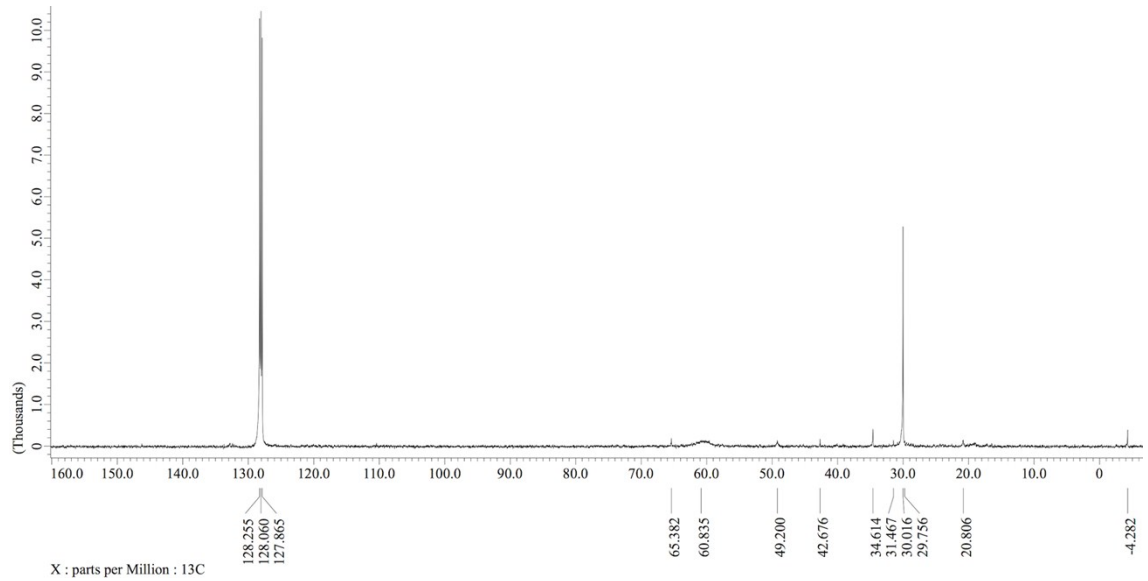

Figure S32. ^{13}C{^{1}H} NMR spectrum of **4-^{13}C** (126 MHz, in benzene-d_6, at 300 K).

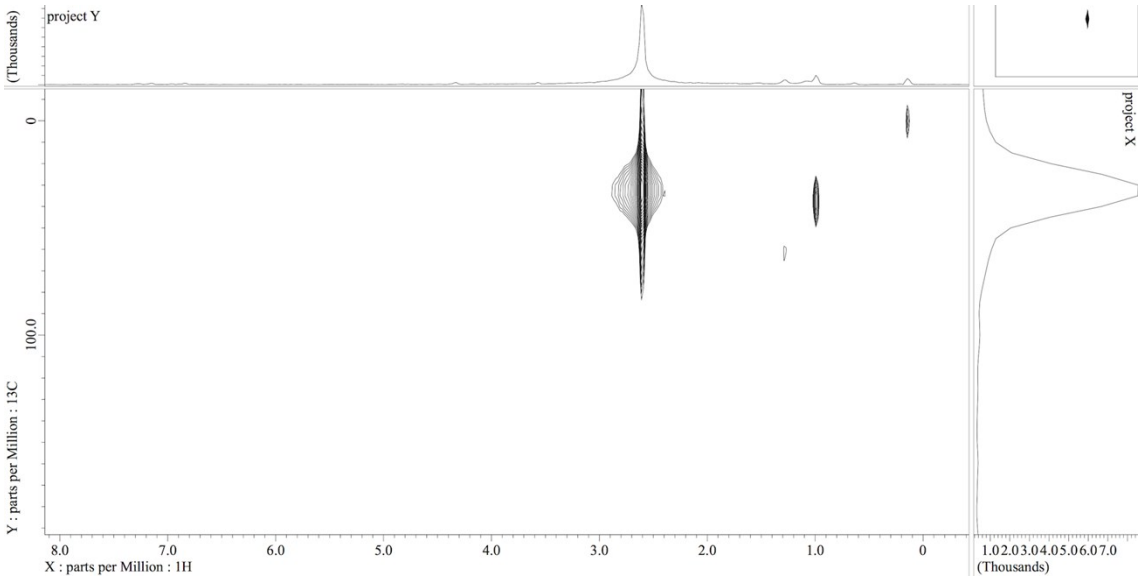

Figure S33. ^{1}H-^{13}C HMQC spectrum of **4-^{13}C** (500 MHz, in benzene-d_6, at 300 K).

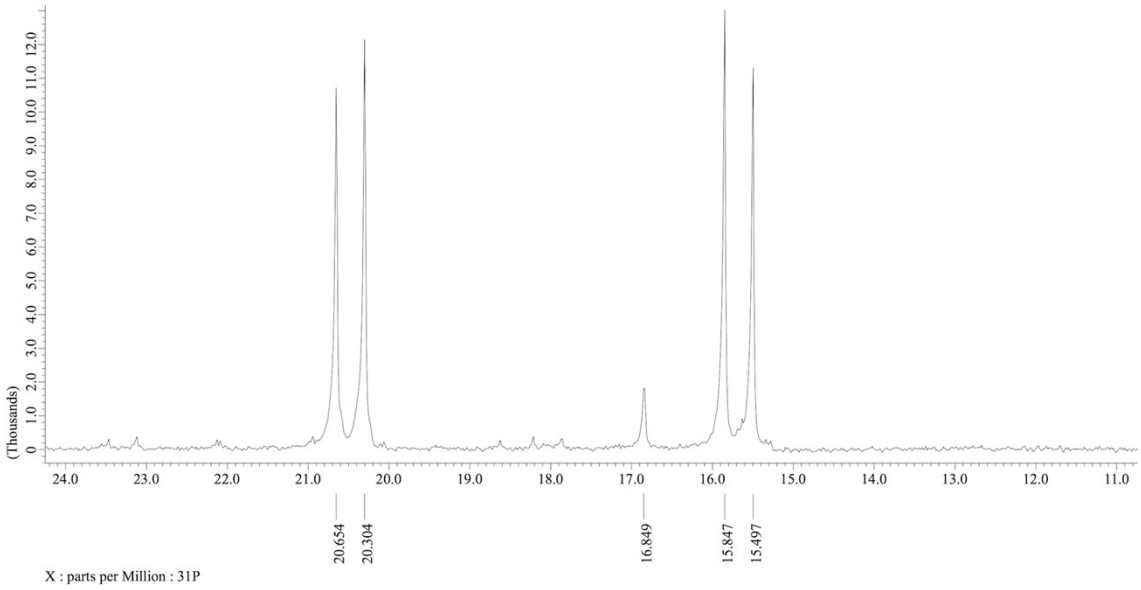

Figure S34. ^{31}P{^{1}H} NMR spectrum of **4-^{13}C** (162 MHz, in benzene-d_6, at 300 K).

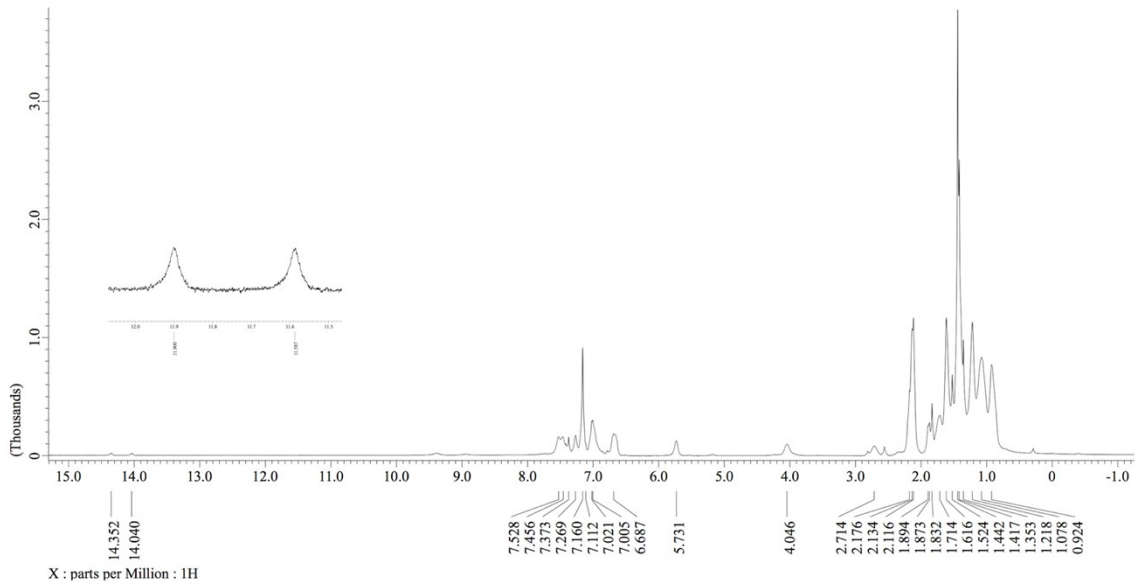

Figure S35. ^{1}H NMR spectrum of benzene-d_6 solution of **3-^{13}C** and **5-^{13}C** (400 MHz, in benzene-d_6, at 300 K).

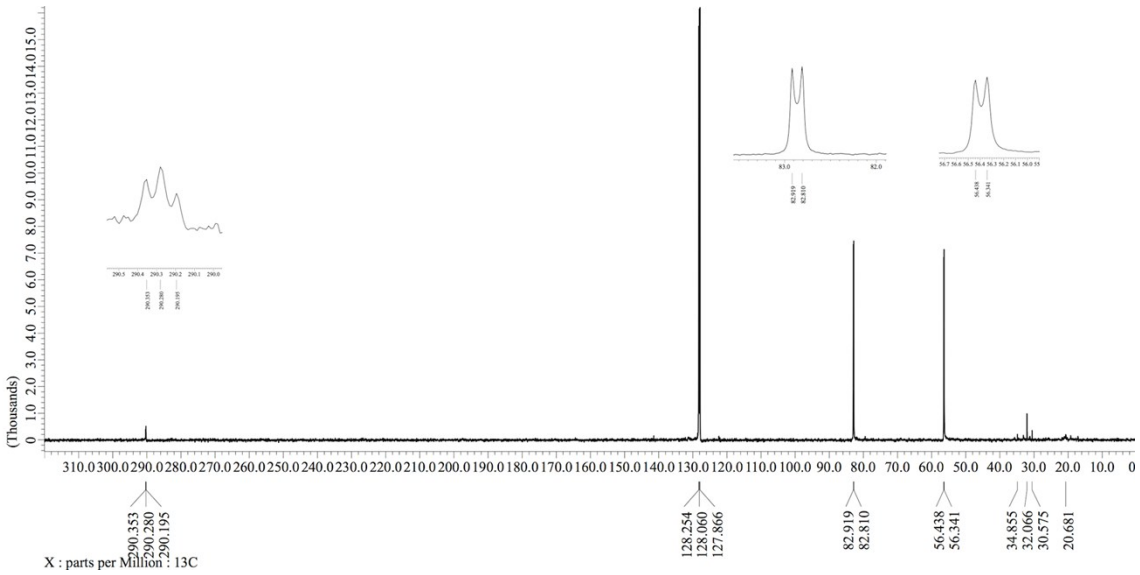

Figure S36. ^{13}C{^{1}H} NMR spectrum of **3-^{13}C** and **5-^{13}C** (400 MHz, in benzene-d_6, at 300 K).

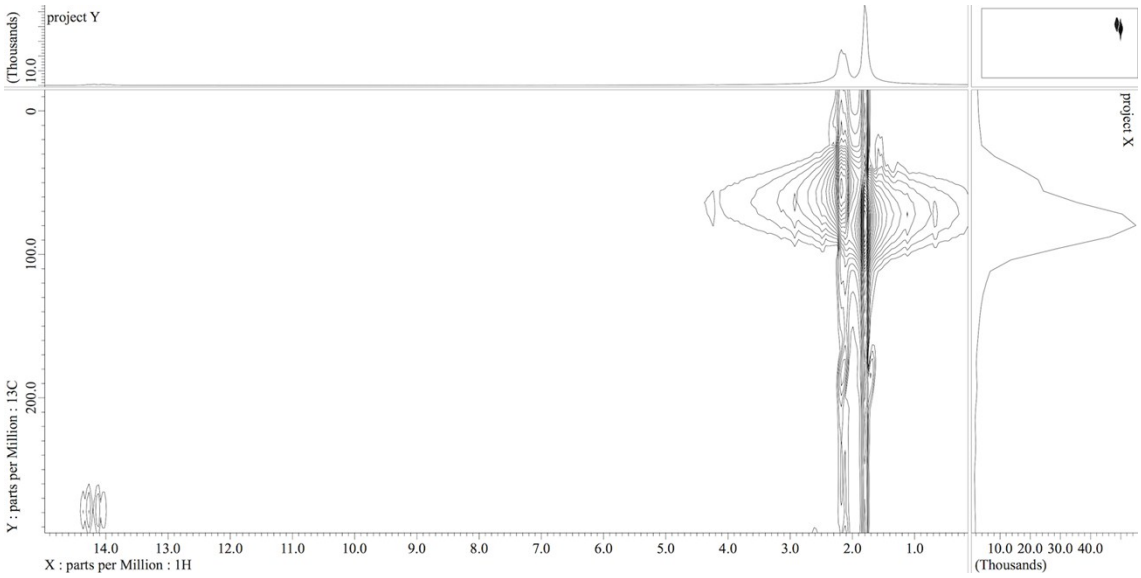

Figure S37. ^{1}H-^{13}C HMQC spectrum of **3-^{13}C** and **5-^{13}C** (500 MHz, in benzene-d_6, at 300 K).

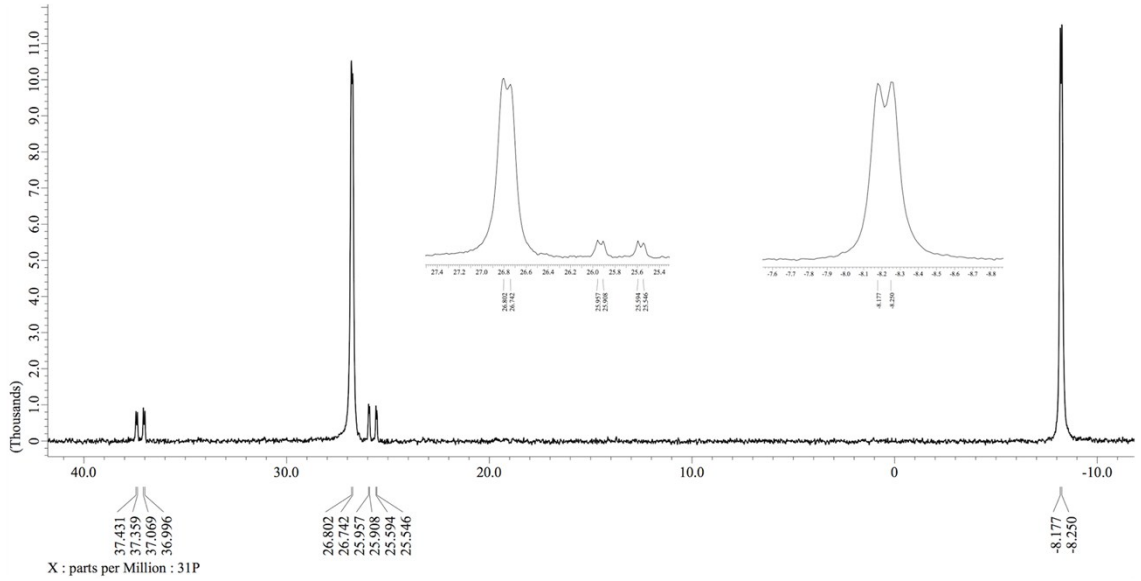

Figure S38. ^{31}P{^{1}H} NMR spectrum of **3-^{13}C** and **5-^{13}C** (162 MHz, in benzene-d_6, at 300 K).

Figure S39. ^{13}C-^{13}C EXSY spectrum of **3-^{13}C** (100 MHz, in benzene-d_6, at 300 K, Mixing time = 10 ms).

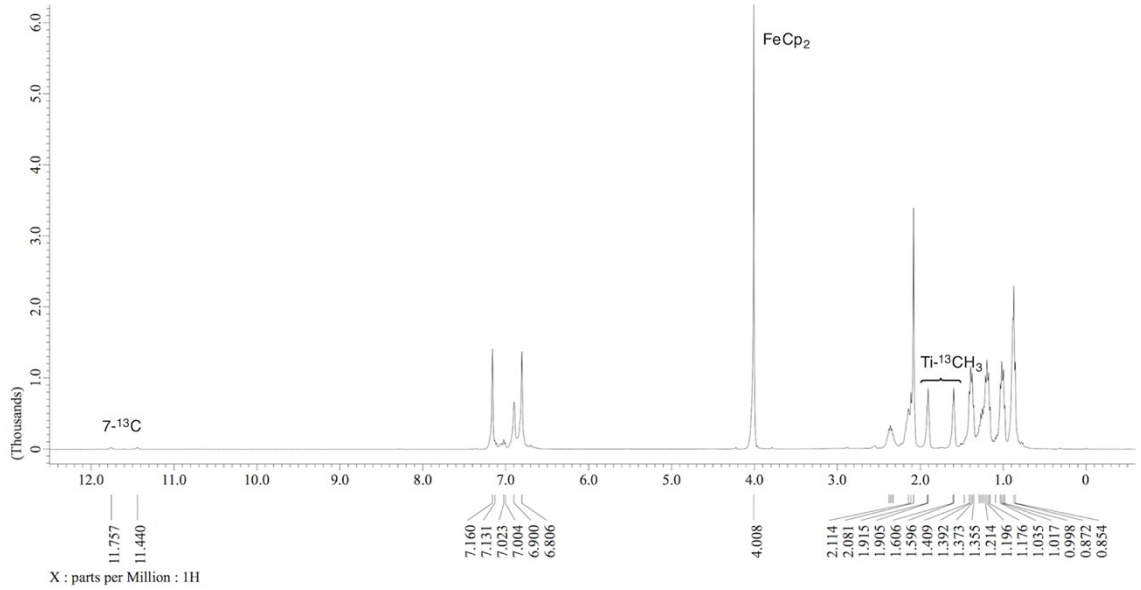

Figure S40. ^{1}H NMR spectrum of benzene-d_6 solution of **6-^{13}C** (400 MHz, in benzene-d_6, at 300 K).

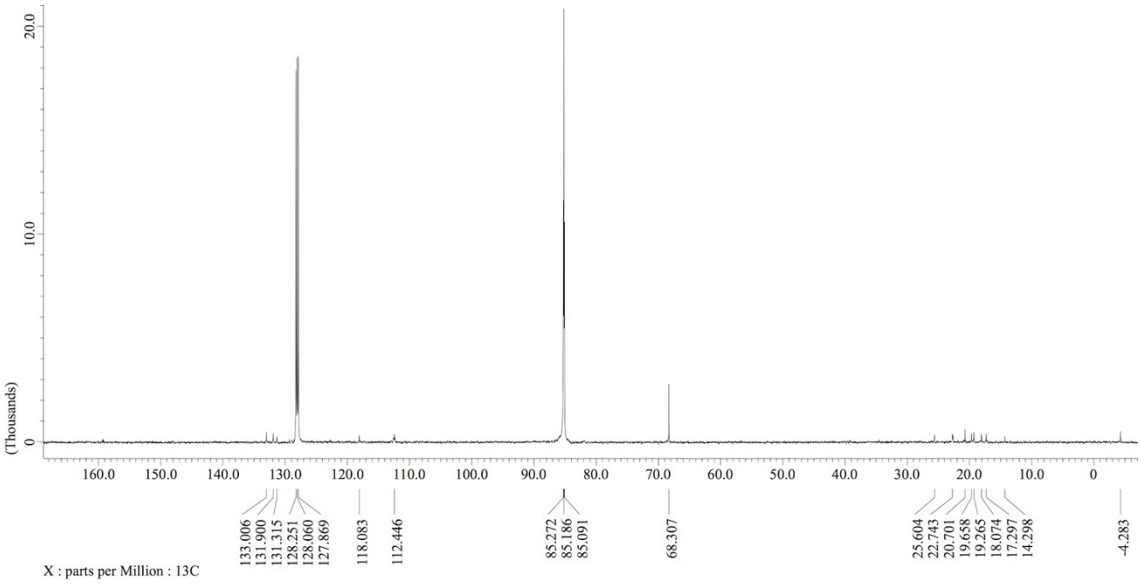

Figure S41. $^{13}C\{^{1}H\}$ NMR spectrum of **6-^{13}C** (400 MHz, in benzene-d_6, at 300 K).

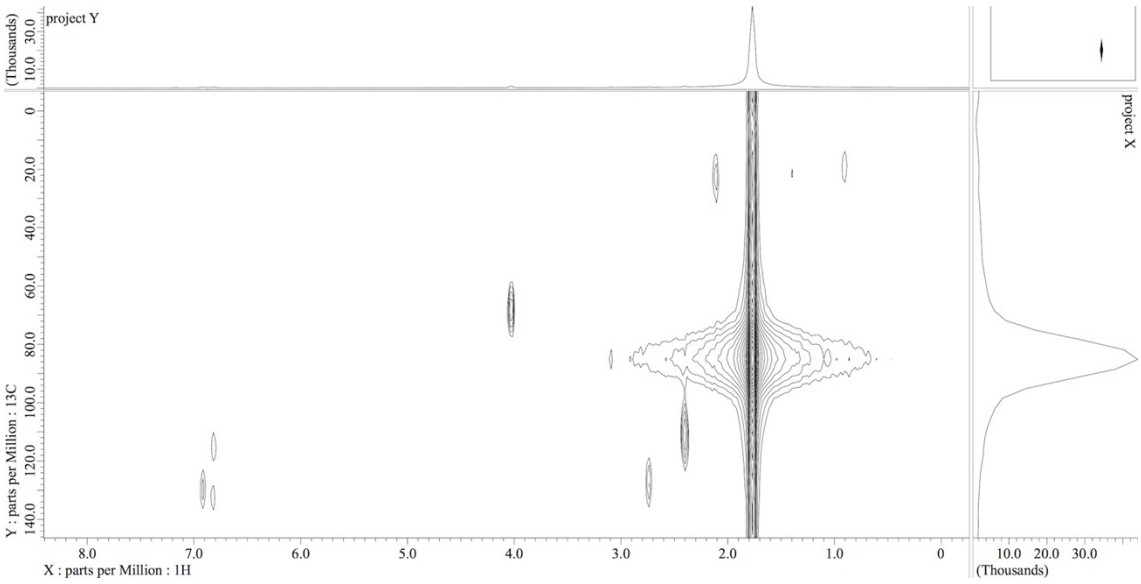

Figure S42. ^{1}H-^{13}C HMQC spectrum of **6-^{13}C** (500 MHz, in benzene-d_6, at 300 K).

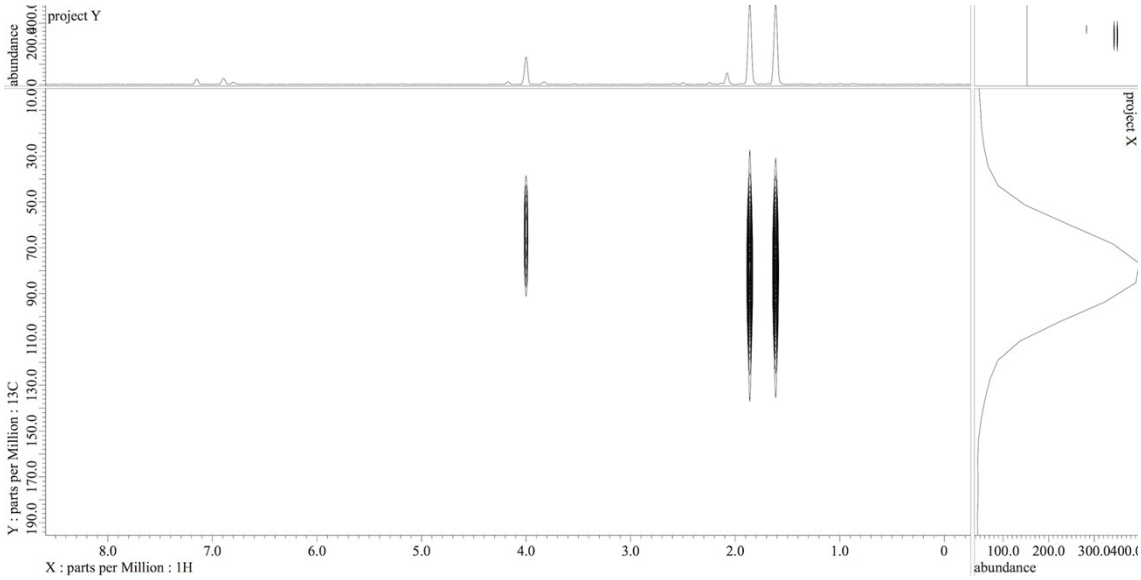

Figure S43. ^{1}H-^{13}C HMBC spectrum of **6-^{13}C** (500 MHz, in benzene-d_6, at 300 K).

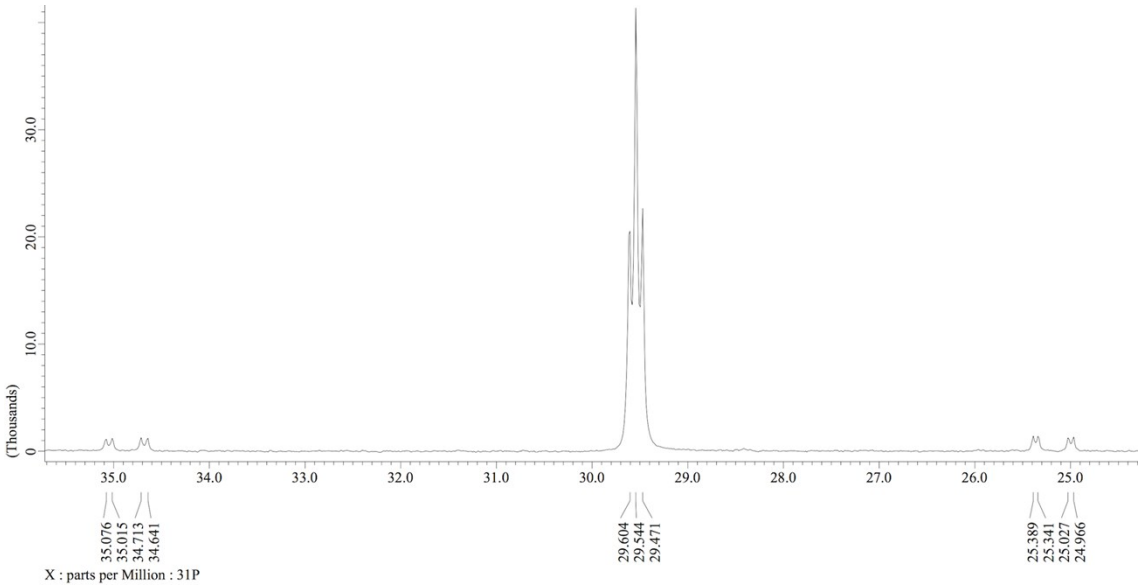

Figure S44. ^{31}P{^{1}H} NMR spectrum of **6-^{13}C** (162 MHz, in benzene-d_6, at 300 K).

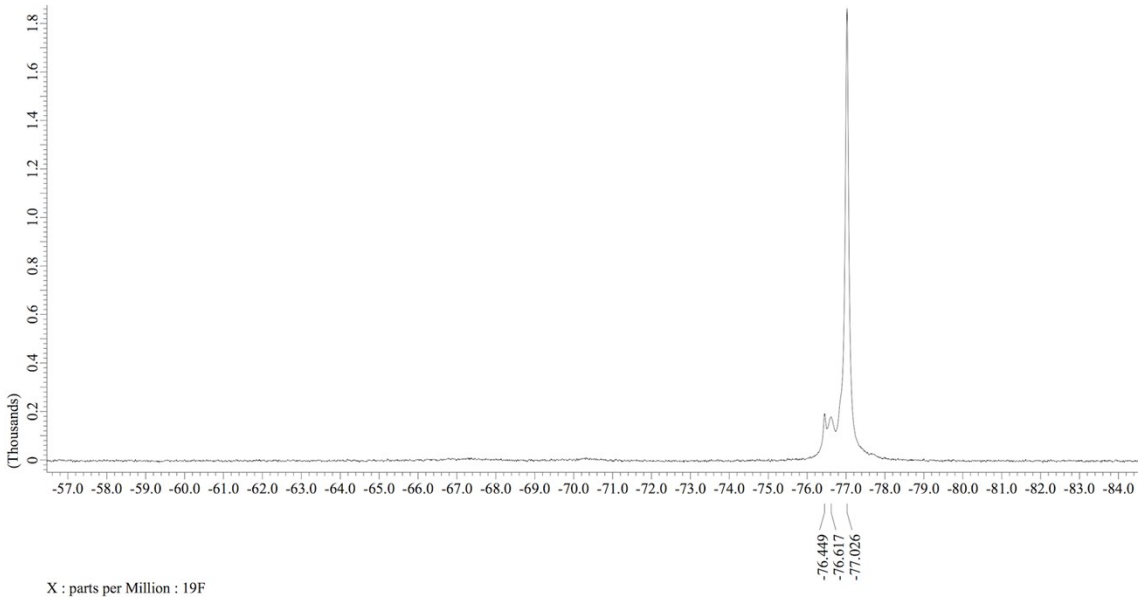

Figure S45. $^{19}F\{^{1}H\}$ NMR spectrum of benzene-d_6 solution of **6-^{13}C** (282 MHz, in benzene-d_6, at 300 K).

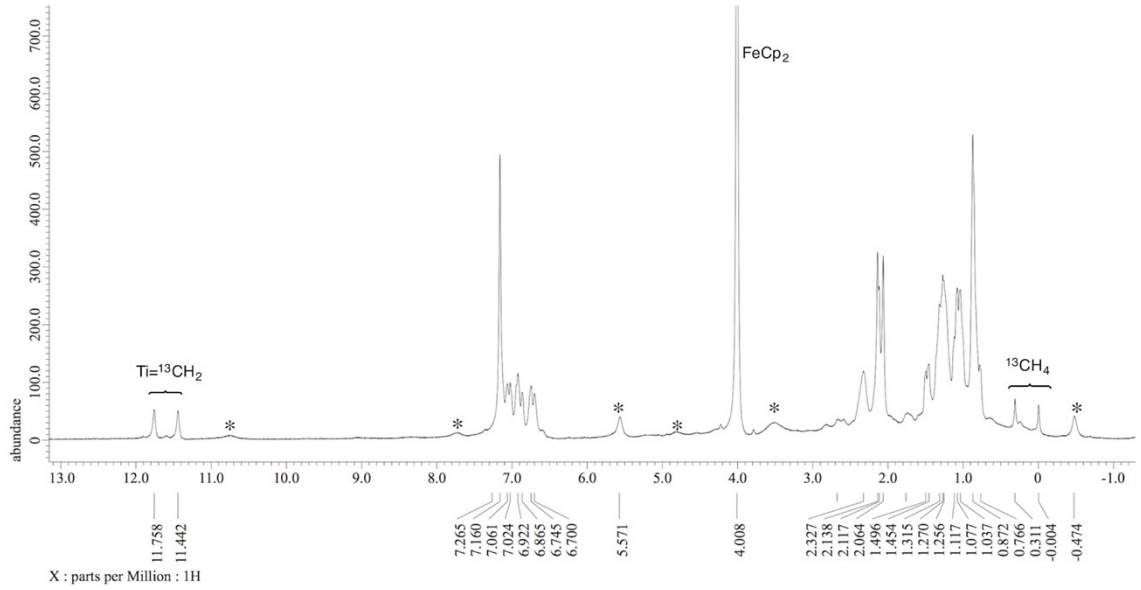

Figure S46. ^{1}H NMR spectrum of benzene-d_6 solution of **7-^{13}C** (400 MHz, in benzene-d_6, at 300 K). *: unidentified products.

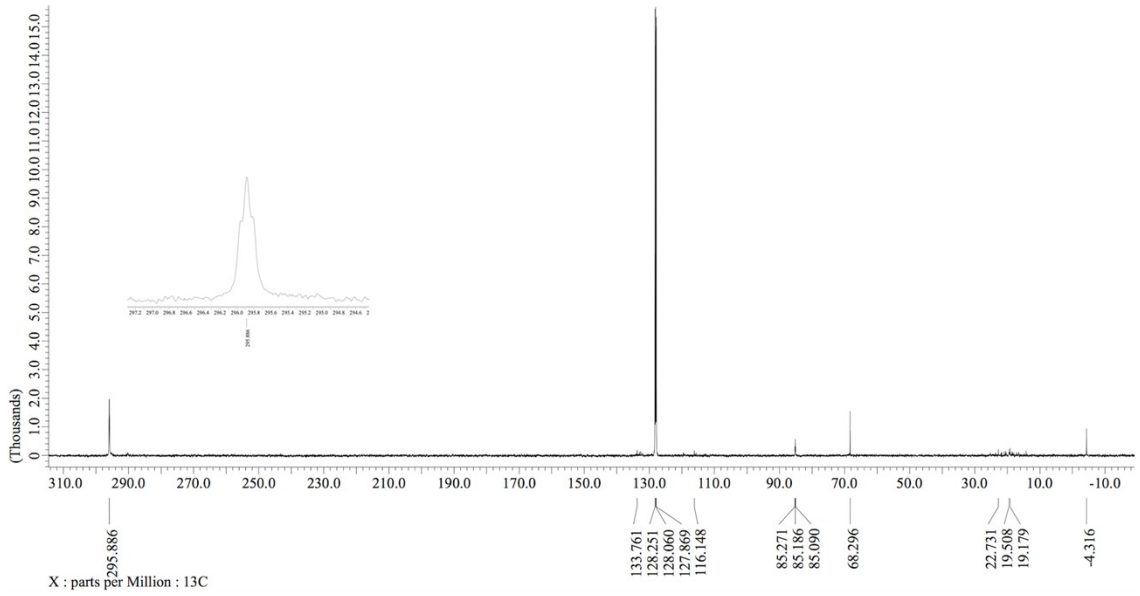

Figure S47. $^{13}C\{^{1}H\}$ NMR spectrum of **7-^{13}C** (400 MHz, in benzene-d_6, at 300 K).

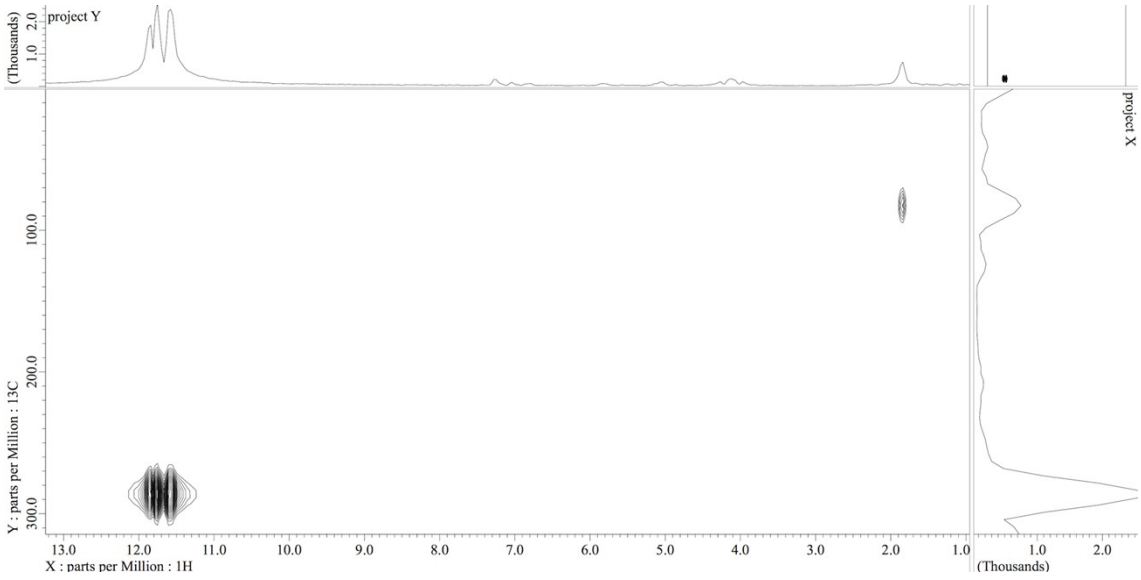

Figure S48. ^{1}H-^{13}C HMQC spectrum of **7-^{13}C** (500 MHz, in benzene-d_6, at 300 K).

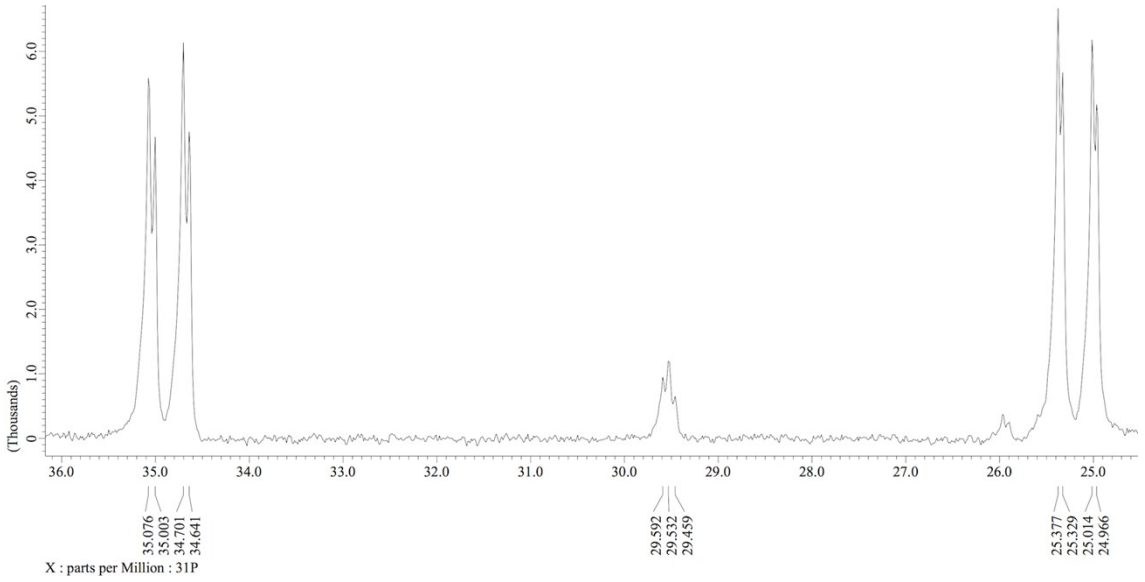

Figure S49. $^{31}P\{^{1}H\}$ NMR spectrum of **7-^{13}C** (162 MHz, in benzene-d_6, at 300 K).

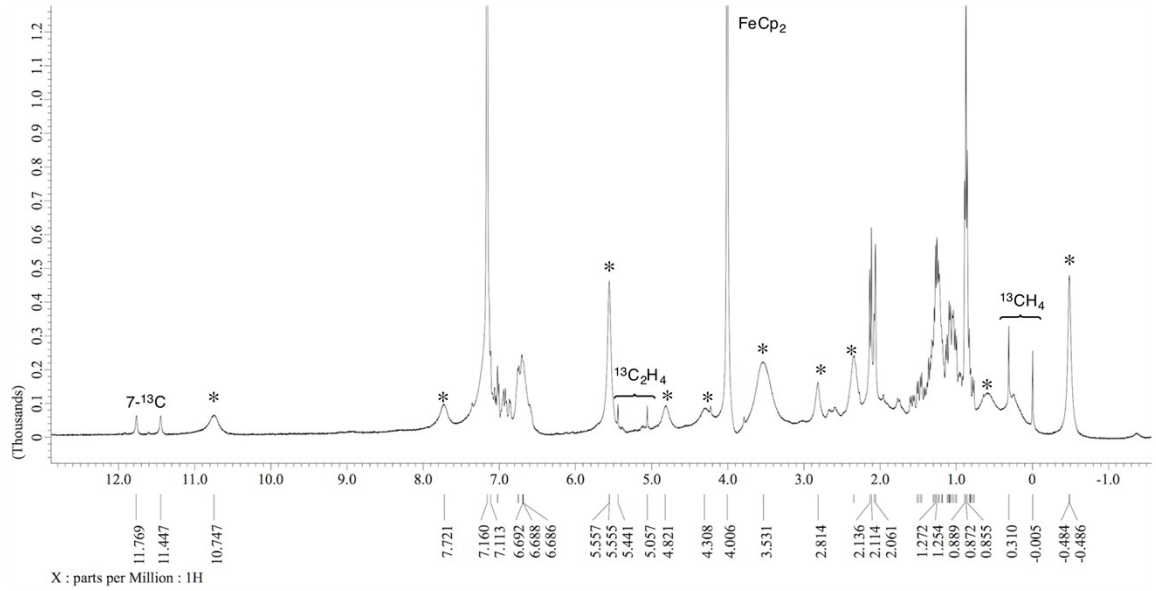

Figure S50. ^{1}H NMR spectrum of benzene-d_6 solution after photolysis of **7-^{13}C** (400 MHz, in benzene-d_6, at 300 K). *: unidentified products.

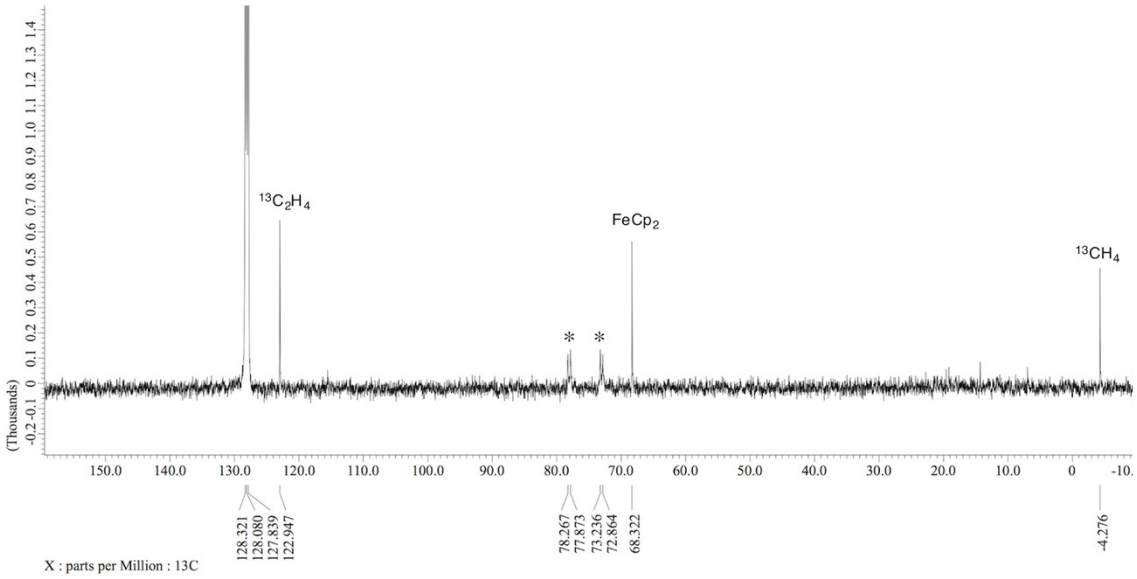

Figure S51. $^{13}C\{^1H\}$ NMR spectrum of benzene-d_6 solution after photolysis of **7-^{13}C** (100 MHz, in benzene-d_6, at 300 K). *: unidentified product.

Cyclic Voltammetry

Cyclic voltammetry measurement of **1** was carried out using an E2 Epsilon (BAS) autolab potentiostat/galvanostat under control by BAS software. A standard three-electrode cell configuration was employed using a glassy carbon working electrode, a platinum wire counter electrode, and a platinum wire as the pseudo-reference electrode. [^{n}Bu$_4$N][PF$_6$] (0.2 M, THF solution) was used as the supporting electrolyte. All electrochemical data are referenced to the [FeCp$_2$]$^+$/[FeCp$_2$] redox couple. In a typical experiment, 15-20 mg of **1** were dissolved in 10 mL of 0.2 M THF solution containing electrolyte. As a note, complex 1 is poorly soluble in the solution.

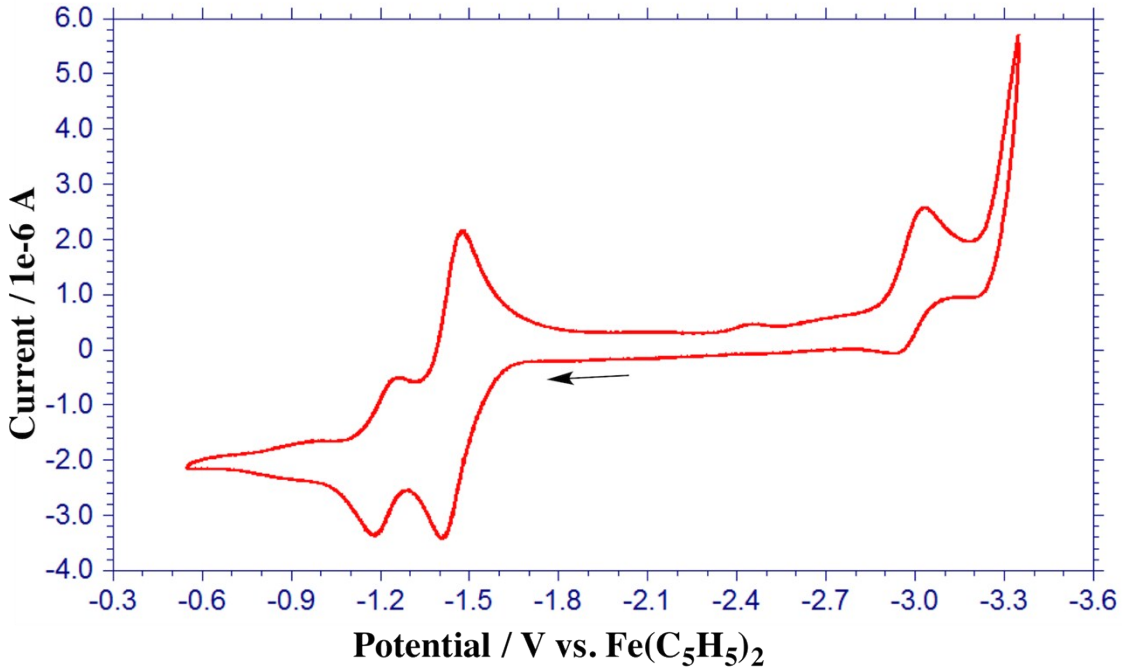

Figure S52. Cyclic Voltammogram of **1** (0.2 M [^{n}Bu$_4$N][PF$_6$] in THF (referenced to FeCp$_2^{0/+}$ at 0.0 V), 0.10 V s^{-1} scan rate, at 300 K). $E_{1/2}$ = –1.45 V, $E_{1/2}$ = –1.22 V, E = –3.03 V.

X-ray Crystallography

Crystallographic data are summarized Table S1-S2. Suitable crystals for X-ray analysis of **2** and **6** were placed on the end of a Cryoloop coated in NVH oil. The X-ray intensity data collection was carried out on a Bruker D8QUEST CMOS area detector for **2** and a Bruker APEXII CCD area detector for **6** using graphite-monochromated Mo-Kα radiation (λ = 0.71073 Å) at 100(1) K. Preliminary indexing was performed from a series of twenty-four (**2**) or thirty-six (**6**) 0.5° rotation frames with exposures of 10 seconds. Rotation frames were integrated using SAINT,[5] producing a listing of non-averaged F^2 and $\sigma(F^2)$ values which were then passed to the SHELXTL[6] program package for further processing and structure solution. The intensity data were corrected for Lorentz and polarization effects and for absorption using SADABS.[7] All calculations were performed using SHELXS[8] and SHELXL.[9] These structures were solved by Patterson and Fourier transform methods. All reflections were used during refinement. Non-hydrogen atoms were refined anisotropically and hydrogen atoms were refined using riding models. For **2**, one site occupied by pentane was identified in the asymmetric unit. This site was considerably disordered and was treated by SQUEEZE as a diffuse contribution.[10] In the resulting void space, a contribution of 53 e^- per unit cell was found and taken to represent 0.5 pentane in the asymmetric unit for each Ti complex. For **6**, the pentane molecule was disordered over two positions. The thermal ellipsoids were fixed by SHELXL restraints, DELU and SIMU.

These results were checked using the IUCR's CheckCIF routine. The alerts in the output are related to the disordered groups and crystal solvents. The large values of the second parameter on the SHELXL weighting are due to the poor quality of crystals.

Table S1. Summary of Structure Determination of 2·(pentane)$_{0.5}$

Empirical formula	$C_{39.5}H_{70}N_2OP_2Ti$
Formula weight	698.81
Temperature	100(2) K
Wavelength	0.71073 Å
Crystal system	*Tricilinic*
Space group	*P***Error!** (No. 2)
Cell constants:	
a	11.965(8) Å
b	12.501(9) Å
c	16.775(11) Å
α	69.62(2) °
β	86.44(3) °
γ	64.68(3) °
Volume	2115(3) Å^3
Z	2
Density (calculated)	1.097 Mg/m^3
Absorption coefficient	0.307 mm^{-1}
F(000)	762
Crystal size	0.22 x 0.22 x 0.09 mm^3
Theta range for data collection	3.06 to 27.66 °
Index ranges	$-15 \le h \le 15$, $-15 \le k \le 16$, $-21 \le l \le 21$
Reflections collected	54095
Independent reflections	9762 [*R* (int) = 0.0668]
Completeness to theta = 27.55°	98.9 %
Absorption correction	Semi-empirical from equivalents
Max. and min. transmission	0.7456 and 0.7051
Refinement method	Full-matrix least-squares on F^2
Data / restraints / parameters	9762 / 0 / 404
Goodness-of-fit on F^2	1.039
Final R indices [I>2sigma(I)]	R_1 = 0.0479, wR_2 = 0.1081
R indices (all data)	R_1 = 0.0684, wR_2 = 0.1174
Largest diff. peak and hole	0.597 and -0.406 e.Å^{-3}

Table S2. Summary of Structure Determination of 6·(pentane)

Empirical formula	$C_{34}H_{58}F_3N_3O_3P_2STi$
Formula weight	727.71
Temperature	100(1) K
Wavelength	0.71073 Å
Crystal system	*Monoclinic*
Space group	$P2_1/n$ (No. 14)
Cell constants:	
a	15.1311(10) Å
b	18.4016(12) Å
c	15.2549(10) Å
α	90 °
β	111.107(4) °
γ	90 °
Volume	3962.6(5) $Å^3$
Z	4
Density (calculated)	1.220 Mg/m^3
Absorption coefficient	0.395 mm^{-1}
F(000)	1552
Crystal size	0.20 x 0.08 x 0.07 mm^3
Theta range for data collection	2.37 to 27.49 °
Index ranges	$-18 \le h \le 19$, $-23 \le k \le 23$, $-19 \le l \le 19$
Reflections collected	99023
Independent reflections	9150 [R (int) = 0.1081]
Completeness to theta = 27.55°	99.8 %
Absorption correction	Semi-empirical from equivalents
Max. and min. transmission	0.7456 and 0.6256
Refinement method	Full-matrix least-squares on F^2
Data / restraints / parameters	9150 / 67 / 446
Goodness-of-fit on F^2	1.025
Final R indices [I>2sigma(I)]	R_1 = 0.0552, wR_2 = 0.1337
R indices (all data)	R_1 = 0.1337, wR_2 = 0.1584
Largest diff. peak and hole	0.789 and -0.439 $e.Å^{-3}$

References

[1] (a) B. C. Bailey, J. C. Huffman, D. J. Mindiola, W. Weng and O. V. Ozerov, *Organometallics*, 2005, **24**, 1390. (b) B. C. Bailey, H. Fan, E. W. Baum, J. C. Huffman, M.-H. Baik and D. J. Mindiola, *J. Am. Chem. Soc.*, 2005, **127**, 16016.

[2] N. T. Jones, S. T. Liddle, C. Wilson and P. L. Arnold, *Organometallics*, 2007, **26**, 755.

[3] V. W. Manner, T. F. Markle, J. H. Freudenthal, J. P. Roth and J. M. Mayer, *Chem. Commun.*, 2008, 256.

[4] J. J. Curley, R. G. Bergman and T. D. Tilley, *Dalton Trans.*, 2012, **41**, 192.

[5] *SAINT*; Bruker AXS Inc.: Madison, WI, USA. 2009.

[6] *SHELXTL*; Bruker AXS Inc.: Madison, WI, USA, 2009.

[7] G. M. Sheldrick, *SADABS*; University of Gottingen: Germany, 2007.

[8] (a) G. M. Sheldrick, *Acta Crystallogr.*, 2008, **A64**, 112. (b) G. M. Sheldrick, *Acta Crystallogr.*, 2015, **C71**, 3.

[9] $R_1 = \Sigma||F_o| - |F_c|| / \Sigma |F_o|$, $wR_2 = [\Sigma w(F_o^2 - F_c^2)^2/\Sigma w(F_o^2)^2]^{½}$, $GOF = [\Sigma w(F_o^2 - F_c^2)^2/(n - p)]^{½}$;where n = the number of reflections and p = the number of parameters refined.

[10] (a) P. van der Sluis, A. L. Spek, *Acta Crystallogr.*, 1990, **A46**, 194. (b) A. L. Spek, *Acta Crystallogr.*, 2009, **D65**, 148. (c) A. L. Spek, *Acta Crystallogr.*, 2015, **C71**, 9.